Inherently lean rats have enhanced activity and skeletal muscle response to central melanocortin receptors

Authors:

Chaitanya K. Gavini[1, 2], Steven L. Britton[3,4], Lauren G. Koch[3], Colleen M. Novak[1, 5]

[1]School of Biomedical Sciences, Kent State University, Kent, Ohio, USA.

[2]Department of Cell and Molecular Physiology, Stritch School of Medicine, Loyola University Chicago, Maywood, Illinois, USA.

[3]Department of Anesthesiology, University of Michigan, Ann Arbor, Michigan, USA.

[4]Department of Molecular and Integrative Physiology, University of Michigan, Ann Arbor, Michigan, USA.

[5]Department of Biological Sciences, Kent State University, Kent, Ohio, USA.

Keywords:

High- and low-capacity runners (HCR. LCR), energy expenditure, obesity, skeletal muscle

Running Head: VMH melanocortins and activity energy expenditure

Corresponding author:

Correspondence should be addressed to Chaitanya K. Gavini, Department of Cell and Molecular Physiology, Stritch School of Medicine, Loyola University Chicago, 2160 S. First Ave, Maywood, IL 60153, USA. Tel: +1 708 216 7936; email: cgavini@luc.edu

Word count: 3287

Funding:

This work was funded by National Institutes of Health (NIH) grants NIH R01NS055859 and NIH R15DK097644, as well as American Heart Association grant 12GRNT12050566 to CMN. The LCR-HCR rat model system was funded by the Office of Research Infrastructure Programs grant P40OD021331 (to LGK and SLB) from the National Institutes of Health.

Disclosure:

The authors declare no conflict of interest.

STUDY IMPORTANCE:

- Intra-ventromedial hypothalamic melanocortin receptor activation increases physical activity and energy expenditure
- Here, we demonstrate that this response is enhanced in inherently lean rats
- Intrinsic differences in brain melanocortins and sympathetic outflow to muscle may underlie the elevated activity energy expenditure seen in leanness

ABSTRACT

Objective

Activity thermogenesis and energy expenditure (EE) are elevated in intrinsically lean rats (high-capacity runners, HCR), and are also stimulated by melanocortin receptor activation in the ventromedial hypothalamus (VMH). Here, we determined if HCR are more responsive to central modulation of activity EE compared to low-capacity runners (LCR).

Methods

HCR and LCR rats received intra-VMH microinjections of Melanotan II (MTII), a mixed melanocortin receptor agonist. Changes in EE, respiratory exchange ratio (RER), activity EE, muscle heat, norepinephrine turnover (NETO), and muscle energetic modulators were compared.

Results

HCR were significantly more responsive to intra-VMH MTII-induced changes in EE, activity EE, NETO to some muscle subgroups, and muscle mRNA expression of some energetic modulators. Though HCR had high muscle activity thermogenesis, limited MTII-induced modulation of muscle thermogenesis during activity was seen in LCR only.

Conclusions

An inherently lean, high-capacity rat phenotype showed elevated response to central melanocortin stimulation of activity EE and use of fat as fuel. This may be driven by sympathetic outflow to skeletal muscle, which was elevated after MTII. Central melanocortin receptor activation also altered skeletal muscle energetic modulators in a manner consistent with elevated EE and lowered RER.

INTRODUCTION

Genetic and environmental factors interact to influence energy balance. One characteristic that differs with leanness is physical activity, a heritable trait that varies widely between individuals in both humans and rodents[1,2,3]. Across species, intrinsic aerobic capacity predicts high physical activity, health, longevity, and a favorable metabolic profile[4,5,6,7,8,9,10,11]. Rats selectively bred as high capacity runners (HCR) are more physically active than their counterparts selectively bred as low capacity runners (LCR). LCR are prone to weight gain, obesity, and cardiovascular disorders[6,12], and HCR have a low adiposity, high activity (independent of differences in body weight[13]), and high energy expenditure (EE) relative to body size[13]. The high EE seen in HCR is predominantly due to heightened non-resting EE[13], which persists even during controlled activity, indicating low economy of activity—more kcal used for the same workload—in the HCR[12,13]. This implicates skeletal muscle energetic and thermogenic mechanisms, which may stem from the enhanced sympathetic drive observed in HCR[13].

The elevated activity, EE, SNS drive, and muscle expression of energetic mediators characteristic of HCR are also modulated by central melanocortin receptors[14,15,16], suggesting a melanocortinergic mechanism for the muscle energetic phenotype of HCR. Like brain melanocortins, the ventromedial hypothalamus (VMH) plays an important role in fuel allocation[15,16,17,18]. Activation of VMH melanocortin receptors using a non-specific agonist Melanotan II (MTII) increases EE and physical activity, and decreases respiratory exchange ratio (RER), switching fuel preference to fats; it lowers fuel economy during activity where 'wasted' calories are dissipated as heat[14]. HCR and LCR respond differently to central melanocortins[19,20], a system known to modulate sympathetic drive[15,16,21]. Here, we examine how VMH melanocortin

receptors alter activity-related EE, heat dissipation, SNS drive, and molecular mediators of energy homeostasis in lean (HCR) and obesity-prone (LCR) rats, predicting that increased EE and thermogenesis will be reflected in augmented activation at each level of this brain-muscle pathway.

METHODS

Adult male HCR/LCR rats (N=104, 52/group, generation 32 and 34) from the University of Michigan were individually housed on a 12:12 light:dark cycle (lights on at 0700 EST) and received food (5P00 MRH 3000) and water *ad libitum*. All studies were approved by the Kent State University IACUC.

Stereotaxic surgery and transponder implantation

Stereotaxic surgeries were performed to chronically implant guide cannulae aimed at the VMH[14]. Briefly, rats (total N=86 for cannulation) were anesthetized using isoflurane and mounted on a stereotaxic apparatus using atraumatic ear bars. The VMH was targeted using the coordinates: anterior-posterior, -2.5mm; medial-lateral, +0.5mm; dorsal-ventral, -6mm (from dura), and an injection needle with 3mm projection (final dorsal-ventral, -9mm from dura). After completion of the study, rats with guide cannulae within 250μm of the VMH (N=74 accurate placements) were used for data analysis as shown in our previous studies[14,20]. In 24 male HCR/LCR (12/group) during stereotaxic surgery, sterile IPTT-300 temperature transponders (Bio Medic Data Systems, Inc.) were implanted on interscapular brown adipose tissue (BAT) and adjacent to gastrocnemius muscle bilaterally.

Body composition and energy expenditure

Body composition was measured using an EchoMRI-700 (EchoMRI, Houston, TX) to determine the fat and lean mass (in grams) of each rat the day before experiments. This did not interfere with transponder function. After 24-48hrs of acclimation in testing cages, EE and physical activity were measured using small-animal indirect calorimetry (4-chamber Oxymax FAST system, Columbus Instruments, Columbus, OH) at thermoneutral conditions, as previously reported[13,14]. Rats were injected either with the nonspecific melanocortin receptor agonist MTII (20pmoles/200nl) or vehicle (aCSF, 200nl)[14]. The first 15 min of data was not included in the analysis. EE data (VO_2, VCO_2, RER, kcal/hr) were averaged, and physical activity data were expressed as mean beam breaks/minute. In all EE and thermogenesis studies described here, all rats received counterbalanced vehicle and MTII injections separated by at least four days, with each rat acting as its own control thereby nullifying the effect of body weight and composition[22,23]. For EE, analysis of covariate was used to account for differences in body composition.

To assess locomotor efficiency, physical-activity EE was measured using gas exchange during a treadmill activity test; MTII-induced physical activity precluded accurate measurement of resting EE. At least one day after a 15-min treadmill acclimation period, rats were placed in the treadmill after injections of either MTII (20pmoles/200nl) or vehicle (aCSF) and allowed to acclimate without food for 2 hrs. Rats then walked on the treadmill at 7 m/min for 30 min while activity-EE data were collected every 10 sec. All EE data from both studies were analyzed using 2x2 mixed ANOVA using SPSS, with ANOVA significance set at $p < 0.05$ unless otherwise stated.

Muscle temperature

Skeletal muscle and BAT heat dissipation were measured every 15 min for 4 hrs after intra-VMH MTII or vehicle microinjection, with BAT thermogenesis as a positive control. In a separate experiment, rats received microinjections of either MTII or vehicle 1.5 hrs prior to measurement of skeletal muscle heat dissipation during controlled physical activity on a treadmill. Gastrocnemius temperatures in each leg were recorded at baseline (before injecting and immediately before treadmill walking) and at set intervals during a 35-min, 5-level graded treadmill test as reported previously[13,14]. Data from each study were analyzed using 3-way ANOVAs.

Norepinephrine turnover (NETO)

Norepinephrine (NE) turnover (NETO) was used to assess sympathetic drive to peripheral tissues including liver, heart, BAT, skeletal muscle (including quadriceps, lateral and medial gastrocnemius, EDL, and soleus), and WAT depots (mesenteric (MWAT), gluteal (GWAT), retroperitoneal (RWAT), inguinal (IWAT), and epididymal WAT (EWAT)) in HCR and LCR. NETO was measured using α-methyl-p-tyrosine (aMPT in saline vehicle) as previously reported[24,25]. HCR and LCR were divided into 3 groups (aMPT/MTII, aMPT/aCSF-vehicle, control; n=8/group). On the day of the study, food was removed and assigned rats were given aMPT injections (125 mg aMPT/kg body weight; 25 mg/ml) 2 and 4 hrs before tissue collection; 30 minutes after the first aMPT injection, rats received intra-VMH MTII or vehicle. All rats were euthanized by rapid decapitation between 1200 and 1500 EST (5-8 hrs after lights-on), 4 hours after the first aMPT injection. Tissues were rapidly dissected and snap-frozen in liquid nitrogen. Catecholamines were isolated from homogenized tissue and measured using HPLC, as

previously described[13,14,24,25]. NETO was calculated:

k = (lg[NE]0 – lg[NE]4)/(0.434 x 4)

K = k[NE]0

k is the constant rate of NE efflux (also known as fractional turnover rate),

[NE]0 is the initial NE concentration or from 0-hr group (control),

[NE]4 is the final NE concentration or from 4-hr group (aMPT-MTII/ aMPT-vehicle), and

K = NETO.

Differences in tissue NETO between intra-VMH MTII-microinjected and vehicle-microinjected rats were calculated with respect to control-group rats; NETO/gram tissue/hour was compared using a 2x2 mixed ANOVA.

mRNA and protein expression

Skeletal muscle (gastrocnemius and quadriceps), liver, MWAT, and BAT were collected from HCR/LCR rats (N=32, 16/group) 4hrs after intra-VMH microinjection of either MTII or vehicle (N=8/treatment). Tissue samples were homogenized and total mRNA extracted as previously reported[13,14], and compared to glyceraldehyde 3-phosphate dehydrogenase (GAPDH) using the comparative Ct method (ΔCt). See Supplementary Material for list of primers. Protein was isolated from tissue homogenate[13,14] and compared using Western blots. Primary and secondary antibodies (see Supplementary Material) were diluted in blocking buffer according to manufacturer instructions and developed using a chemiluminescence detector using an Amersham kit (GE Healthcare, UK). Data are expressed as a percent expression using samples from vehicle-treated HCR rats as the reference value (defined as 100%) relative to GAPDH (for mRNA) or actin (for protein), and were analyzed using 2x2 mixed ANOVA. As we were

specifically interested in the magnitude of effect of MTII in HCR vs. LCR, we used planned *(a priori)* comparisons using t-tests with a Bonferroni correction (two t-tests with $p<0.025$).

RESULTS

For body weight and composition, LCR were consistently larger with more fat and lean mass than HCR. Some slight but significant differences were found between treatments (Table S1). Statistical results are listed in Tables S2-S16, with data expressed as mean ± SEM.

EE in HCR was more responsive to intra-VMH MTII

As shown in Figure 1A-D, intra-VMH MTII significantly increased EE, VO_2, and physical activity (horizontal and ambulatory), with a significantly greater response in HCR (significant interaction), and lowered RER in both HCR and LCR. HCR had higher activity (all dimensions), VO_2, and VCO_2. MTII also increased treadmill-activity EE and VO_2 (Figure 1E-H); MTII decreased RER more in LCR than HCR (Figure 1G). HCR showed a greater MTII-induced increase in treadmill-activity EE (Figure 1H). There were significant interactions between treatment and HCR/LCR for free-moving EE and treadmill-activity EE, using either body weight or lean mass as covariates. Treadmill-walking EE showed main effects where HCR had lower EE and RER, and a trend toward higher treadmill VO_2.

Muscle heat dissipation

As described in the Supplementary Material, during resting, compared to vehicle, MTII induced an increase in BAT temperature, and the change in temperature from baseline was significantly higher after MTII treatment (compared to vehicle) between 30min and 120min after injection

(Figure S1). There were no significant differences in BAT response to MTII between HCR and LCR. Compared to vehicle, intra-VMH MTII did not significantly increase gastrocnemius muscle temperatures or elevation relative to baseline (Figure S2). Compared to vehicle injections, MTII injections induced higher treadmill activity-associated gastrocnemius temperatures in LCR (Figure 2A, B). Consistent with previous findings[13], lean HCR had a greater change in treadmill locomotion-induced skeletal muscle heat dissipation during treadmill locomotion under both vehicle- and MTII-injected conditions compared to obesity-prone LCR (Figure 2B).

Intra-VMH MTII microinjection differentially elevated sympathetic drive to metabolic tissues in lean vs. obesity-prone rats

Compared to vehicle, intra-VMH MTII induced a significant increase in SNS drive to skeletal muscle of both lean HCR and obesity-prone LCR, although HCR were significantly more affected (significant interaction) than LCR in soleus, quadriceps, and lateral gastrocnemius (Figure 3). Intra-VMH MTII also induced a significant increase in SNS drive to all WAT depots examined, BAT, heart, and liver (Figure 3, Table 1). MTII-induced NETO was greater in HCR than in LCR (significant interaction) for MWAT, GWAT, and IWAT, as well as for BAT and liver (Table 1). In heart, both baseline and MTII-induced NETO was greater in LCR than HCR, with a significant interaction where LCR showed a greater response to MTII (Figure 3F). Compared to vehicle-treated LCR, vehicle-treated HCR had higher NETO in skeletal muscle, BAT, and MWAT, consistent with previous baseline findings for skeletal muscle and BAT[13].

Intra-VMH MTII elevated expression of mRNA of mediators of energy expenditure

Levels of mRNA expression of potential molecular mediators of energy balance are shown in Table 2 and Figure 3. Compared to vehicle-treated HCR, gastrocnemius muscle of intra-VMH MTII-treated HCR had significantly higher mRNA expression of UCP2, UCP3, PGC-1α, PPARα, PPARδ, PPARγ, SERCA1, SERCA2, and β_2 AR, and a significant decrease in Kir6.2 (Figure 4A). Gastrocnemius showed a significantly higher expression of UCP2, UCP3, PPARα, PPARγ, and SERCA2 in MTII-treated LCR than vehicle-treated LCR. In quadriceps, MTII- and vehicle-microinjected HCR differed in mRNA expression (MTII>vehicle, within HCR) of UCP2, UCP3, PPARα, PPARδ, SERCA1, and SERCA2 (Figure 4B). MTII-treated LCR quadriceps showed significantly higher mRNA expression of UCP2 and UCP3 (Figure 4B) compared to vehicle-treated LCR quadriceps.

Compared to vehicle-treated rats, HCR but not LCR with intra-VMH MTII microinjections had significantly elevated mRNA expression of UCP1, PGC-1α, PPARδ, PPARγ, and PPARα in BAT (Table 2). Compared to vehicle, intra-VMH MTII also induced a significant increase in mRNA expression of PPARγ, PPARα, and PPARδ in WAT of intra-VMH MTII treated HCR where LCR showed MTII-induced increase in mRNA expression of PPARα and PPARδ in WAT. In liver, intra-VMH MTII-treated HCR showed significantly higher mRNA expression of UCP2, PPARα, PPARδ, PPARγ, and PGC-1α compared to vehicle-treated HCR. In LCR liver, MTII- and vehicle-treated rats significantly differed in mRNA expression of PPARα, PPARδ, PPARγ, and PGC-1α.

As shown in Table 3 and Figure S3, protein expression of mediators of EE did not consistently change in accordance with mRNA expression. In quadriceps, MTII-treated HCR only showed

trends in pAMPK, pACC, PPARγ, and SERCA1. No significant differences or trends were found in protein expression with intra-VMH MTII in LCR. In gastrocnemius, intra-VMH MTII-microinjected HCR showed significantly higher expression of PGC-1α, pAMPK, and pACC compared to vehicle-treated HCR, with trends in other mediators; no significant differences were found in LCR (Figure S3).

As shown in Table 3 and Figure S3, in BAT of HCR, MTII-treated rats showed significantly higher UCP1, PGC-1α, pAMPK, and pACC. No significant differences were observed with MTII in LCR. No significant differences were observed with MTII in WAT except in pAMPK in MTII-treated HCR compared to vehicle-treated HCR. In liver, MTII-microinjected HCR showed significantly more pACC and pAMPK; no significant differences were observed in LCR.

DISCUSSION

Phenotypic leanness associated with high intrinsic aerobic capacity in rats is coupled with elevated total EE, and the predominant source of this is activity-related EE stemming from high daily physical activity along with low economy of activity in these rats[12,13]. This low muscle work efficiency suggests wasting of calories to a greater extent in HCR than LCR, potentially modulated by enhanced sympathetic drive and altered expression of molecular mediators of energy conservation and expenditure observed in HCR[13]. These phenotypic differences were similar to those seen in response to intra-VMH melanocortin receptor activation[14], suggesting an elevated response of the melanocortinergic VMH-SNS-muscle axis in the lean HCR. Here, we identified a phenotype-linked increase in EE, physical activity, activity-associated EE, and VO_2 after site-specific activation of central melanocortin receptors. Many of these energetic changes

were amplified in lean HCR compared to obesity-prone LCR; for example, VMH melanocortin receptor activation had a greater impact on EE and VO_2 in HCR (Figure 1), even taking into account differences in body weight and composition. The melanocortin receptor stimulation of EE during low- and moderate-intensity physical activity implicates mechanistic changes impacting muscle work efficiency, particularly in the lean HCR. This stems in part from enhanced central activation of SNS outflow to muscle. Elevated functioning of this brain-SNS-muscle axis in the high-capacity phenotype may be an important factor promoting aerobic capacity and potentially leanness.

Some thermogenic changes accompanied the MTII-induced increase in EE. BAT thermogenesis showed a short-term increase in freely moving MTII-treated rats (Figure S1). MTII enhanced treadmill-walking gastrocnemius muscle temperature, but contrary to expectation, obesity-prone LCR showed a greater response in their muscle heat dissipation during activity, approaching the level of vehicle-treated HCR (Figure 2). Prior reports indicate that during activity, EE and muscle thermogenesis rise alongside each other, are similarly enhanced by central stimuli[14], and are suppressed in concert after weight loss[26]. Muscle thermogenesis plateaus at relatively low levels of exertion[13,14,26,27]. This implies that, mechanistically, heat dissipation does not fully correspond to calorie use in muscle, particularly at higher workloads. Given the high muscle activity thermogenesis seen in HCR[13], central MTII may enhance EE without being reflected in further incremental increases in muscle temperature (i.e., subject to a ceiling effect). Our data also suggest that melanocortin stimulation can be used to enhance or normalize activity thermogenesis even in the obesity prone.

Activity thermogenesis and skeletal muscle metabolism are important in maintaining leanness[28], and this may be driven in part through central modulation. Evidence implicates a pathway through which the VMH and central melanocortin system integrate central and peripheral metabolic cues to meet muscle energy and glucose needs[15,16,29] though modulation of the SNS[16,30]. Here, we found that activation of VMH melanocortin receptors increased sympathetic outflow to peripheral metabolic systems in both HCR and LCR (Figure 3; Table 1). Moreover, in some muscle subgroups, NETO was significantly more enhanced by MTII in HCR compared to obesity-prone LCR. Differences in central autonomic regulation could therefore contribute to the overall higher SNS drive seen in the lean HCR[13]. The exception was the heart, where the MTII-induced increase in sympathetic outflow was higher in the LCR, and LCR showed higher NETO both with and without central melanocortin receptor stimulation (Figure 3). This corresponds with evidence that HCR are protected against hypertension[6] and with the role of melanocortin peptides and receptors in sympathetically driven hypertension and against the hypertensive effects of MTII[21,31,32]. The enhanced responsiveness of SNS outflow to muscle in HCR supports the idea that the amplified metabolic response to central melanocortins in HCR are due in part to higher SNS stimulation of muscle. This, along with muscle response to SNS signaling[33], may underlie the phenotypic differences in fuel economy and the associated changes in cellular energy mediators in the periphery.

Overall, these findings affirmed our previous identification of phenotype-dependent differences in HCR and LCR[13] as well as muscle response to central melanocortin receptor activation[14]. Central melanocortin activation was effective in modulating mRNA expression in BAT and liver in both HCR and LCR (Figure 4, Table 2); here, we focus primarily on muscle, specifically on

mediators of thermogenesis, fatty acid metabolism, and energy conservation. Potential thermogenic mediators SERCA1 & 2 and UCP2 & 3 showed induced mRNA expression in quadriceps and oxidative gastrocnemius muscle with central melanocortin stimulation, with some elevation seen in HCR and not LCR (gastrocnemius SERCA1, quadriceps SERCA 1 & 2; Table 3). Conversely, mRNA expression of MED1 and components of ATP-gated K^+ channels were higher in LCR muscle, potentially contributing to their overall lower muscle temperatures[35] and their energy conservation. Similar to previous reports[13,34], central melanocortin stimulation induced mRNA expression of PGC-1α, PPARα, PPARγ, and PPARδ in oxidative gastrocnemius muscle, and PPARα, PPARδ in quadriceps, with many of these significant in HCR but not LCR (Figure 4). These changes may be responsible for the central melanocortin receptor-induced increase in EE and decrease in RER. While the 4-hr time course of the study was optimal to detect increases in mRNA expression, it likely obscured detection of suppressive effects of central MTII beyond one instance (Kir6.2 in HCR gastrocnemius; Figure 4) and some statistical trends (PPARα, pAMPK, PPARγ and pACC; Table 3). Also, the time course did not allow for adequate time for detection of altered protein expression. Most of the changes identified were phosphorylation related and did not require translation. The expression of the activated form of AMPK (pAMPK) may underlie the ability of central MTII to upregulate fatty acid oxidation and reduce RER through its regulation of ACC and CPT1[36]. Lastly, both mRNA and protein expression reinforced our previous findings[13] showing baseline differences between HCR and LCR reflecting the observed phenotype-dependent differences in activity-related EE, RER, and muscle energy use. Taken together with the MTII-induced changes demonstrated here and the proposed melanocortin-activated VMH-SNS-muscle pathway, this suggests phenotypic differences in myocyte responsiveness to adrenergic stimuli, consistent with the findings of

Lessard et al., 2009[33].

Altogether, our data demonstrate that melanocortin receptors in the VMH activate SNS outflow, increasing sympathetic drive to skeletal muscle, modulate fuel allocation and use through differential activation of molecular mediators of energy homeostasis, and increase EE while lowering fuel economy of activity. We have also demonstrated that functioning of this axis is heightened at every level in HCR compared to LCR—activation of melanocortin receptors in the VMH increases energy use in peripheral tissues including muscle, with a stronger effect in the high-capacity phenotype[13,14]. It is likely that muscle fuel uptake and utilization is modulated through the SNS, affecting skeletal muscle or other metabolically active tissues. The central melanocortin system, differentially expressed in the lean HCR and obese LCR, is known to impact muscle lipid mobilization and glucose uptake in the periphery via the SNS[15,17,19,20,37,38]. These findings support the importance of central modulation of SNS outflow to muscle in modulating activity EE, and suggest that differences in this pathway are linked to a high-aerobic capacity phenotype that shows obesity resistance. We speculate that running capacity, leanness, and skeletal muscle energy use and thermogenesis are coupled mechanistically. These results implicate this pathway as a potential mechanism underlying high-endurance-associated low economy of activity and leanness, and may help identify potential mediators that can be targeted to alter energy balance equation towards negative energy balance.

ACKNOWLEDGEMENT

We acknowledge the expert care of the rat colony provided by Lori Heckenkamp and Shelby Raupp. Contact LGK lgkoch@umich.edu or SLB brittons@umich.edu for information on the LCR and HCR rats: these rat models are maintained as an international resource with support from the Department of Anesthesiology at the University of Michigan, Ann Arbor, Michigan. We would like to thank Lydia Heemstra for organizing personnel, Amber Titus for a critical reading of the manuscript, and the staff of the animal care and housing at Kent State University for their support in taking care of the animals.

FIGURE LEGENDS

Figure 1: High-capacity runners (HCR) were more responsive to the ability of intra-ventromedial hypothalamic (VMH) melanocortin receptor activation to enhance activity-related energy expenditure (EE). Low-capacity runners (LCR) and HCR were given intra-VMH microinjections of the mixed melanocortin receptor agonist Melanotan II (MTII; gray bars) or vehicle (Veh; black bars). Over 4 hours, with a significant interaction where HCR responded more than LCR, intra-VMH MTII significantly increased free-moving EE (A), VO_2 (B), and physical activity (D), while decreasing respiratory exchange ratio (RER) similarly in HCR and LCR (C). (E-H) Intra-VMH MTII also induced changes in EE and RER in rats walking on a treadmill at 7 meters/min for 30 min. MTII increased activity-associated EE (E) and VO_2 (F), and decreased RER (G) in HCR and LCR. HCR showed lower overall walking-induced RER, while intra-VMH MTII produced a larger RER decrease in LCR than HCR (G), whereas HCR were more responsive to MTII-induced enhancement of activity EE (H). *within group, MTII treatment significantly different from veh; **HCR significantly different from LCR within treatment; $p<0.05$. (N=10)

Figure 2: (A) Low and moderate intensity treadmill activity increased skeletal muscle (gastrocnemius) temperature in high-capacity runners (HCR; circles) and low-capacity runners (LCR; triangles) after intra-ventromedial hypothalamic (VMH) microinjections of the mixed melanocortin receptor agonist Melanotan II (MTII; open symbols) or vehicle (Veh; filled symbols). (B) Walking-induced increases in muscle temperature from baseline were significantly higher in HCR, whereas intra-VMH MTII significantly increased activity-associated muscle heat dissipation in LCR but not HCR. *LCR, MTII treatment significantly different from Veh; **

HCR > LCR, main effect (A) and difference at baseline (B); $p<0.05$. (N=10/HCR, 6/LCR)

Figure 3: Norepinephrine turnover (NETO) showed differences in sympathetic drive in high- and low-capacity runners (HCR. LCR) after intra-ventromedial hypothalamic (VMH) microinjections of the mixed melanocortin receptor agonist Melanotan II (MTII; gray bars) or vehicle (Veh; black bars). Intra-VMH MTII significantly increased NETO in skeletal muscle including (A) medial gastrocnemius, (B) lateral gastrocnemius, (C) quadriceps, (D) soleus, and (E) extensor digitorum longus (EDL); HCR showed significantly higher NETO in each of these muscle groups, and also had significantly greater MTII-induced NETO in lateral gastrocnemius, quadriceps, and soleus (line x treatment interaction). (F) Intra-VMH MTII also increased NETO in heart, but here the MTII-induced increase was greater in LCR than HCR. *within group, MTII treatment significantly different from veh; **HCR significantly different from LCR within treatment; $p<0.05$. (N=7/HCR, 8/LCR)

Figure 4: Intra-ventromedial hypothalamic (VMH) microinjections of the Melanotan II (MTII) altered mRNA expression of energetic mediators in skeletal muscle (A: medial gastrocnemius; B: quadriceps) in high-and low-capacity runners (HCR, LCR). Beta2: β2 adrenergic receptor; UCP2 and 3: uncoupling protein 2 and 3; PPARa, d, and g: peroxisome proliferator-activated receptor α, δ, and γ; SERCA 1 and 2: sarco/endoplasmic reticulum ATPase 1 and 2; Kir6.1 and 6.1: subunits of the ATP-gated K^+ channel, Med1: mediator of RNA polymerase II transcription subunit 1. HCR-MTII ≠ LCR-MTII in all cases. *within group, MTII treatment significantly different from veh; $p<0.05$. (N=8/group)

REFERENCES

1. Joosen AM, Gielen M, Vlietinck R, Westerterp KR. Genetic analysis of physical activity in twins. *Am J Clin Nutr* 2005;82(6):1253-1259.
2. Levine JA, Kotz CM. NEAT--non-exercise activity thermogenesis--egocentric & geocentric environmental factors vs. biological regulation. *Acta Physiol Scand,* 2005;184(4):309-318.
3. Levine JA, Lanningham-Foster LM, McCrady SK, et al. Interindividual variation in posture allocation: possible role in human obesity. S*cience* 2005;307(5709):584-586.
4. Aspenes ST, Nilsen TI, Skaug EA, Bertheussen GF, Ellingsen O, Vatten L, Wisloff U. Peak oxygen uptake and cardiovascular risk factors in 4631 healthy women and men. *Med Sci Sports Exerc* 2011;43(8):1465-1473.
5. Bray MS. Genomics, genes, and environmental interaction: the role of exercise. *J Appl Physiol* 2000;88(2):788-792.
6. Koch LG, Britton SL, Wisloff U. A rat model system to study complex disease risks, fitness, aging, and longevity. *Trends Cardiovasc Med* 2012;22(2):29-34.
7. Kodama S, Saito K, Tanaka S, Maki M, et al. Cardiorespiratory fitness as a quantitative predictor of all-cause mortality and cardiovascular events in healthy men and women: a meta-analysis. *JAMA* 2009;301(19):2024-2035.
8. Novak CM, Escande C, Gerber SM, et al. Endurance capacity, not body size, determines physical activity levels: role of skeletal muscle PEPCK. *PLoSONE* 2009;4(e5869).
9. Zhan WZ, Swallow JG, Garland T Jr., Proctor DN, Carter PA, Sieck GC. Effects of genetic selection and voluntary activity on the medial gastrocnemius muscle in house mice. *J Appl Physiol* 1999;87(6):2326-2333.

10. Kokkinos P, Myers J, Kokkinos JP, et al. Exercise capacity and mortality in black and white men. *Circulation* 2008;117:614-622.

11. Myers J, Prakash M, Froelicher V, Do D, Partington S, Atwood JE. Exercise capacity and mortality among men referred for exercise testing. *N Engl J Med* 2002;346:793-801.

12. Novak CM, Escande C, Burghardt PR, et al. Spontaneous activity, economy of activity, and resistance to diet-induced obesity in rats bred for high intrinsic aerobic capacity. *Horm Behav* 2010;58(3):355-367.

13. Gavini CK, Mukherjee S, Shukla C, Britton SL, Koch, LG, Shi H, Novak CM. Leanness and Heightened Non-Resting Energy Expenditure: Role of Skeletal Muscle Activity Thermogenesis. *Am J Physiol Endocrinol Metab* 2014;306(6):E635-47.

14. Gavini CK, Jones WC II, Novak CM. Ventromedial hypothalamic melanocortin receptor activation: regulation of activity energy expenditure and skeletal muscle thermogenesis. *J Physiol* 2016;594:5285–5301.

15. Toda C, Shiuchi T, Lee S, et al. Distinct effects of leptin and a melanocortin receptor agonist injected into medial hypothalamic nuclei on glucose uptake in peripheral tissues. *Diabetes* 2009; 58:2757-65.

16. Shiuchi T, Haque MS, Okamoto S, et al. Hypothalamic orexin stimulates feeding-associated glucose utilization in skeletal muscle via sympathetic nervous system. *Cell Metab* 2009;10:466–480.

17. Tanaka T, Masuzaki H, Yasue S, et al. Central melanocortin signaling restores skeletal muscle AMP-activated protein kinase phosphorylation in mice fed a high-fat diet. *Cell Metab* 2007;5:395-402.

18. Miyaki T, Fujikawa T, Kitaoka R, Hirano N, Matsumura S, Fushiki T, Inoue K.

Noradrenergic projections to the ventromedial hypothalamus regulate fat metabolism during endurance exercise. *Neuroscience* 2011;190:239-50.

19. Shukla C, Britton SL, Koch LG, Novak CM. Region-specific differences in brain melanocortin receptors in rats of the lean phenotype. *Neuroreport* 2012;23:596-600.
20. Shukla C, Koch LG, Britton SL, Cai M, Hruby VJ, Bednarek M, Novak CM . Contribution of regional brain melanocortin receptor subtypes to elevated activity energy expenditure in lean, active rats. *Neuroscience* 2015;310:252-67.
21. Rahmouni K, Haynes WG, Morgan DA, Mark AL. Role of melanocortin-4 receptors in mediating renal sympathoactivation to leptin and insulin. *J. Neurosci* 2003;23:5998–6004.
22. Schoeller DA, Jefford G. Determinants of the energy costs of light activities: inferences for interpreting doubly labeled water data. *Int J Obes Relat Metab Disord* 2002;26 (1):97-101.
23. Tschöp MH, Speakman JR, Arch JR, et al. A guide to analysis of mouse energy metabolism. *Nat. Methods* 2012;9:57–63.
24. Shi H, Bowers RR, Bartness TJ. Norepinephrine turnover in brown and white adipose tissue after partial lipectomy. *Physiol Behav* 2004;81:535–42.
25. Vaughan CH, Shrestha YB, Bartness TJ. Characterization of a novel melanocortin receptor-containing node in the SNS outflow circuitry to brown adipose tissue involved in thermogenesis. *Brain Res* 2011;1411:17-27.
26. Almundarij TI, Gavini CK, Novak CM. Suppressed sympathetic outflow to skeletal muscle, muscle thermogenesis, and activity energy expenditure with calorie restriction. *Physiol Rep.* 2017 Feb;5(4). pii:e13171.

27. Yoo Y, LaPradd M, Kline H, et al. Exercise activates compensatory thermoregulatory reaction in rats: a modeling study. *J Appl Physiol.* 2015;119(12):1400-10.

28. Jensen MD. Fatty acid oxidation in human skeletal muscle. *J Clin Invest* 2002;110:1607–1609.

29. Braun TP, Marks DL. Hypothalamic regulation of muscle metabolism. *Curr Opin Clin Nutr Metab Care* 2011;14(3):237-242.

30. Lindberg D, Chen P, Li C. Conditional viral tracing reveals that steroidogenic factor 1-positive neurons of the dorsomedial subdivision of the ventromedial hypothalamus project to autonomic centers of the hypothalamus and hindbrain. *J Comp Neurol* 2013;521(14):3167-3190.

31. da Silva AA, do Carmo JM, Kanyicska B, Dubinion J, Brandon E, Hall JE. Endogenous melanocortin system activity contributes to the elevated arterial pressure in spontaneously hypertensive rats. *Hypertension* 2008;51(4):884-890.

32. Haynes WG, Morgan DA, Djalali A, Sivitz WI, Mark AL. Interactions between the melanocortin system and leptin in control of sympathetic nerve traffic. *Hypertension* 1999;33(1 Pt 2):542-547.

33. Lessard SJ, Rivas DA, Chen ZP, et al. Impaired skeletal muscle beta-adrenergic activation and lipolysis are associated with whole-body insulin resistance in rats bred for low intrinsic exercise capacity. *Endocrinology* 2009;150(11):4883-4891.

34. Overmyer KA, Evans CR, Qi NR, et al. Maximal oxidative capacity during exercise is associated with skeletal muscle fuel selection and dynamic changes in mitochondrial protein acetylation. *Cell metabolism* 2015;21:468–478.

35. Alekseev AE, Reyes S, Yamada S, et al. Sarcolemmal ATP-sensitive K(+) channels

control energy expenditure determining body weight. *Cell Metab* 2010;11(1):58-69.

36. Minokoshi Y, Kim YB, Peroni OD, Fryer LG, Muller C, Carling D, Kahn BB. Leptin stimulates fatty-acid oxidation by activating AMP-activated protein kinase. *Nature* 2002;415(6869):339-343.
37. Nogueiras R, Wiedmer P, Perez-Tilve D, et al. The central melanocortin system directly controls peripheral lipid metabolism. *J Clin Invest* 2007;117(11):3475-3488.
38. Sohn JW, Harris LE, Berglund ED, et al. Melanocortin 4 receptors reciprocally regulate sympathetic and parasympathetic preganglionic neurons. *Cell* 2013;152(3):612-619.

Table 1. Norepinephrine turnover (ng NE/g tissue/hr) in high-capacity runners (HCR) and low-capacity runners (LCR) 4 hrs after intra-ventromedial hypothalamic microinjection of either the mixed melanocortin receptor agonist MTII or vehicle. Mean±SEM

Tissue		HCR		LCR	
		vehicle	MTII*	vehicle	MTII*
White adipose tissue	Mesenteric†**	18.88** ±2.30	38.73** ±4.72	8.39 ±0.71	15.24 ±1.30
	Retroperitoneal	8.04 ±0.70	13.99 ±1.23	6.32 ±0.87	11.34 ±1.56
	Epididymal†**	5.22** ±0.60	7.58** ±0.87	2.05 ±0.11	5.56 ±0.31
	Gluteal†**	4.92 ±0.30	7.95** ±0.49	4.19 ±0.37	4.52 ±0.40
	Inguinal†**	2.29 ±0.19	3.88** ±0.32	1.90 ±0.17	2.43 ±0.22
Brown adipose tissue†**		27.45** ±1.54	62.50** ±3.51	18.36 ±1.06	30.91 ±1.78
Liver†		0.85 ±0.10	2.11** ±0.26	0.66 ±0.06	1.17 ±0.10

HCR, high-capacity runners; LCR, low-capacity runners (N=7/HCR, 8/LCR)

*MTII>vehicle, within line (HCR/LCR) when interaction was significant; all tissues showed main effect of MTII; $p<0.05$

**HCR≠LCR within treatment indicated; main effect of line (HCR/LCR) indicated on tissue; $p<0.05$

†Significant interaction between treatment (vehicle/MTII) and line (HCR/LCR); $p<0.05$

Table 2. Changes in relative mRNA expression after intra-ventromedial hypothalamic treatment with the melanocortin receptor agonist MTII. In percent of vehicle-treated HCR, mean±SEM

Tissue		HCR		LCR	
		vehicle	MTII	vehicle	MTII
Brown Adipose Tissue	B3-AR	100.0±7.6	101±12.8	80.3±5.2	89.6±10.7
	UCP1*,**	100.0±5.1	129±5.1	65.9±7.9	82.6±5.4
	PPARα*,**	100.0±7.1	132±5.8	73.8±6.5	90.7±7.9
	PPARδ**	100.0±8.0	133±5.5	71.8±6.1	87.7±5.8
	PPARγ*,**	100.0±2.0	123±4.7	79.6±4.3	92.7±5.9
	PGC-1α*,**	100.0±9.6	144±10.5	68.3±9.4	89.2±7.9
White Adipose Tissue	B3-AR*,**	100.0±6.3	116.0±10.5	76.9±7.4	85.9±5.5
	UCP2**	100.0±8.9	110.6±8.3	67.9±7.5	73.9±8.7
	PPARα*,**	100.0±5.5	132.4±7.3	67.9±7.9	91.6±4.1
	PPARδ*,**	100.0±9.7	136.5±5.7	65.0±10.1	97.3±7.5
	PPARγ*,**	100.0±8.1	129.7±8.5	72.5±6.9	89.1±8.4
	PGC-1α**	100.0±5.2	112.9±7.6	70.9±9.6	75.6±8.8
Liver	B2-AR*,**	100.0±7.8	117.6±6.9	75.5±5.7	95.4±9.9
	UCP2*,**	100.0±5.3	129.9±8.4	79.5±6.4	95.9±9.8
	PPARα*,**	100.0±8.2	149.7±10.8	78.3±7.0	109.6±6.8
	PPARδ*,**†	100.0±6.2	172.2±7.2	72.4±7.0	111.0±9.6
	PPARγ*,**	100.0±9.5	164.5±15.4	76.2±5.9	115.0±3.5
	PGC-1α*,**	100.0±4.7	159.8±9.8	72.0±6.0	113.0±8.9

HCR, high-capacity runners; LCR, low-capacity runners; B2-AR, beta-2 adrenergic receptor; B3-AR, beta-3 adrenergic receptor; PPAR, peroxisome proliferator activated protein; PGC-1α, PPARγ coactivator-1α; UCP, uncoupling protein. *MTII>vehicle; ** HCR≠LCR †Significant interaction between treatment (vehicle/MTII) and line (HCR/LCR); $p<0.05$. (N=8/group)

Table 3. Changes in relative protein level after intra-ventromedial hypothalamic treatment with the melanocortin receptor agonist MTII. In percent of vehicle-treated HCR, or as a ratio to unphosphorylated protein, mean±SEM.

Tissue		HCR		LCR	
		vehicle	MTII	vehicle	MTII
Gastroc-nemius	B2-AR**	100.0±5.7	111.6±5.9	80.0±5.2	85.7±5.2
	UCP2*,**	100.0±6.3	108.0±6.4	75.4±6.1	78.6±5.5
	UCP3*,**	100.0±5.6	111.4±5.8	74.0±6.2	77.0±5.4
	PPARα**	100.0±5.2	110.0±6.1	79.7±5.2	85.3±5.4
	PPARδ**	100.0±5.9	113.0±6.4	76.5±5.6	86.0±6.8
	PPARγ**	100.0±5.4	116.7±6.4	77.4±5.5	85.3±5.3
	PGC-1α*,**	100.0±5.6	121.6±4.8	71.7±5.4	79.3±5.2
	CPT1	100.0±6.5	111.7±6.0	89.6±6.0	96.9±5.4
	SERCA1*,**	100.0±4.9	116.5±5.8	74.9±5.2	84.0±6.7
	SERCA2**	100.0±6.0	115.9±5.2	69.5±5.2	74.4±5.6
	Kir6.1**	100.0±4.7	97.7±5.6	119.7±4.3	118.0±7.9
	Kir6.2**	100.0±5.9	97.3±4.8	129.7±5.4	129.5±5.7
	MED1**	100.0±5.0	99.9±5.4	131.7±5.6	128.9±5.9
	FAS	100.0±5.7	97.9±5.4	92.6±5.9	92.4±6.0
	CD36 (FAT)**	100.0±6.2	111.0±5.8	82.0±5.4	87.9±6.6
	ACC	100.0±5.4	99.8±5.5	107.9±5.7	104.4±5.5
	pACC*,**	100.0±5.2	121.4±4.9	78.2±5.4	89.5±5.8
	pACC/ACC*,**	100.2±4.5	122.3±5.5	73.0±7.6	87.3±9.8
	AMPK	100.0±5.4	100.5±5.0	99.9±5.7	99.4±5.5
	pAMPK*,**	100.0±5.2	122.0±4.5	97.2±5.5	91.6±5.4
	pAMPK/AMPK*,**	100.4±6.3	123.0±10.6	79.6±6.1	92.2±3.4
Quadriceps	B2-AR**	100.0±6.7	105.9±6.9	83.7±5.2	87.5±6.7
	UCP2**	100.0±6.1	106.6±7.0	74.4±6.4	76.6±5.4
	UCP3**	100.0±5.7	108.4±5.9	73.0±6.8	75.5±5.8
	PPARα**	100.0±	108.0±8.2	85.0±7.4	89.0±5.9
	PPARδ**	100.0±	102.5±6.9	85.5±5.4	84.7±7.8
	PPARγ**	100.0±	112.5±6.5	83.7±5.4	89.1±5.8
	PGC-1α**	100.0±5.3	111.9±5.2	70.2±5.8	76.3±5.9
	CPT1	100.0±6.5	109.9±6.0	92.6±5.7	102.9±5.4
	SERCA1**	100.0±4.9	114.8±5.8	78.5±5.2	87.0±6.7
	SERCA2**	100.0±5.0	110.9±5.2	76.5±5.7	83.7±6.6
	Kir6.1	100.0±5.7	98.3±5.8	112.9±4.2	109.5±6.9
	Kir6.2**	100.0±4.9	96.7±5.9	126.8±4.4	123.2±5.9
	MED1**	100.0±4.7	98.7±5.8	129.8±5.9	127.0±5.0
	FAS	100.0±6.0	98.7±6.4	98.4±5.6	99.4±6.6
	CD36 (FAT) **	100.0±7.2	103.0±6.1	95.8±6.1	86.4±7.6
	ACC	100.0±6.5	99.0±6.0	106.6±5.7	102.9±5.4
	pACC**	100.0±6.0	113.8±4.8	89.4±5.8	96.4±5.9
	pACC/ACC**	100.8±8.1	117.1±11.3	85.3±9.1	93.4±3.3

	AMPK	100.0±7.5	99.5±7.6	99.8±6.8	99.4±5.5
	pAMPK*,**	100.0±5.0	117.0±4.6	98.6±5.5	89.7±5.3
	pAMPK/AMPK**	100.6±7.3	118.2±7.7	79.3±6.7	90.6±5.9
Brown Adipose Tissue	B3-AR**	100.0±6.3	107.4±8.0	76.3±5.5	88.9±7.8
	UCP1*,**	100.0±3.9	119.4±4.0	65.8±4.9	76.2±3.5
	PPARα	100.0±7.4	115.0±9.8	88.2±8.7	95.7±5.6
	PPARδ	100.0±5.9	107.9±6.7	93.8±4.3	98.8±7.5
	PPARγ**	100.0±4.6	106.5±6.8	78.2±6.3	87.9±7.7
	PGC-1α*,**	100.0±5.4	123.2±6.0	78.0±4.3	85.1±7.2
	CPT1	100.0±6.5	112.8±5.3	78.6±5.4	90.4±7.3
	FAS	100.0±6.3	98.9±5.0	100.9±4.8	99.8±5.8
	CD36 (FAT)**	100.0±9.1	102.6±7.3	90.5±6.5	95.4±6.2
	ACC	100.0±7.3	99.5±6.7	103.7±5.7	104.2±7.6
	pACC*,**	100.0±4.3	126.8±7.1	89.4±6.0	99.8±5.3
	pACC/ACC*,**	100.5±5.8	127.3±1.5	86.4±3.8	97.6±9.9
	AMPK	100.0±6.5	98.6±5.3	101.7±3.8	100.4±7.3
	pAMPK*,**	100.0±5.9	138.7±7.3	79.9±5.7	97.3±7.3
	pAMPK/AMPK*,**	100.8±8.4	141.8±11.2	76.9±3.9	97.5±4.0
White Adipose Tissue	B3-AR**	100.0±5.5	109.0±6.0	80.6±4.6	86.0±6.6
	UCP2**	100.0±5.3	106.0±4.4	89.3±4.8	92.7±5.6
	PPARα	100.0±5.3	111.6±5.9	86.4±6.1	94.2±6.9
	PPARδ	100.0±3.5	106.6±4.2	92.8±4.9	99.5±3.7
	PPARγ	100.0±6.5	102.7±8.2	98.6±5.9	100.9±6.4
	PGC-1α**	100.0±5.9	111.4±6.5	91.8±4.4	99.3±7.2
	FAS	100.0±7.6	96.4±7.3	101.9±5.9	99.8±6.2
	CD36 (FAT)	100.0±5.8	99.6±6.5	104.3±6.8	104.1±5.3
	ACC	100.0±6.3	99.9±5.8	104.4±6.2	103.9±6.2
	pACC	100.0±5.8	112.0±4.4	93.8±5.7	105.4±5.7
	pACC/ACC	100.3±2.1	112.9±6.5	90.7±8.9	102.1±7.5
	AMPK	100.0±5.8	99.8±4.2	100.8±5.4	99.9±5.4
	pAMPK*	100.0±5.9	122.7±5.0	98.1±5.6	107.9±5.6
	pAMPK/AMPK	100.7±9.3	125.1±11.1	98.4±8.4	108.3±2.9
Liver	B2-AR**	100.0±5.0	105.8±6.9	80.4±5.4	89.5±5.5
	UCP2**	100.0±5.1	109.8±5.9	79.9±4.6	86.5±5.2
	PPARα	100.0±6.9	113.6±5.7	89.3±5.4	99.1±4.9
	PPARδ**	100.0±6.3	117.6±6.4	83.7±5.2	91.7±5.6
	PPARγ**	100.0±5.4	115.4±5.9	76.8±5.7	85.2±6.3
	PGC-1α**	100.0±5.8	108.4±4.9	86.5±4.8	87.2±5.7
	CPT1	100.0±5.2	105.3±6.4	88.7±5.2	97.0±4.0
	FAS	100.0±5.5	98.5±6.1	100.8±5.2	101.7±5.8
	CD36 (FAT)**	100.0±4.0	95.7±5.4	111.5±4.9	109.8±4.8
	ACC	100.0±6.2	99.5±5.3	104.8±5.2	105.7±6.7
	pACC	100.0±5.4	125.4±6.8	89.3±5.5	94.2±6.7
	pACC/ACC**	101.2±10.5	126.7±2.1	86.6±9.1	90.0±7.5
	AMPK	100.0±5.9	100.0±6.0	100.3±6.1	100.5±5.4
	pAMPK*,**	100.0±5.2	122.7±5.4	89.7±5.2	95.8±5.0
	pAMPK/AMPK**	100.2±4.9	123.1±4.4	90.0±8.4	96.7±10.4

HCR, high-capacity runners; LCR, low-capacity runners; B2-AR, beta-2 adrenergic receptor; B3-AR, beta-3 adrenergic receptor; PPAR, peroxisome proliferator activated protein; PGC-1α, PPARγ coactivator-1α; UCP, uncoupling protein; CPT1, carnitine-palmitoyl transferase 1; SERCA, sarcoplasmic-endoplasmic reticulum calcium ATPase; Kir, inwardly-rectifying potassium channel; MED1, Mediator of RNA polymerase II transcription subunit 1; FAS, fatty acid synthase; CD36/FAT, cluster of differentiation 36/fatty acid translocase; ACC, acetyl-CoA carboxylase; AMPK, AMP-activated protein kinase. *MTII>vehicle; **HCR≠LCR; $p<0.05$

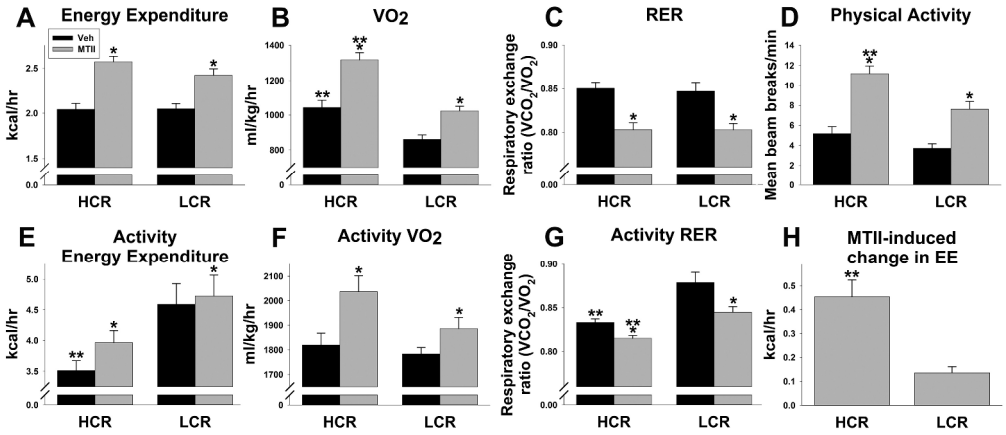

Figure 1: High-capacity runners (HCR) were more responsive to the ability of intra-ventromedial hypothalamic (VMH) melanocortin receptor activation to enhance activity-related energy expenditure (EE). Low-capacity runners (LCR) and HCR were given intra-VMH microinjections of the mixed melanocortin receptor agonist melanotan II (MTII, gray bars) or vehicle (veh; black bars). Over 4 hours, intra-VMH MTII significantly increased free-moving EE (A), VO2 (B), and physical activity (D), while decreasing respiratory exchange ratio (RER; C). HCR showed a significantly greater MTII-induced increase in VO2 and physical activity. Intra-VMH MTII also induced changes in EE and RER in rats walked on a treadmill at 7 meters/min for 30 min. MTII increased activity-associated EE (E) and VO2 (F), and decreased RER (G) in HCR and LCR. HCR showed lower overall walking-induced RER, while intra-VMH MTII produced a larger RER decrease in LCR than HCR (G), whereas HCR were more responsive to MTII-induced enhancement of activity EE (H). *within group, MTII treatment significantly different from veh; **HCR significantly different from LCR within treatment; $p<0.05$. (N=10)

1016x447mm (100 x 100 DPI)

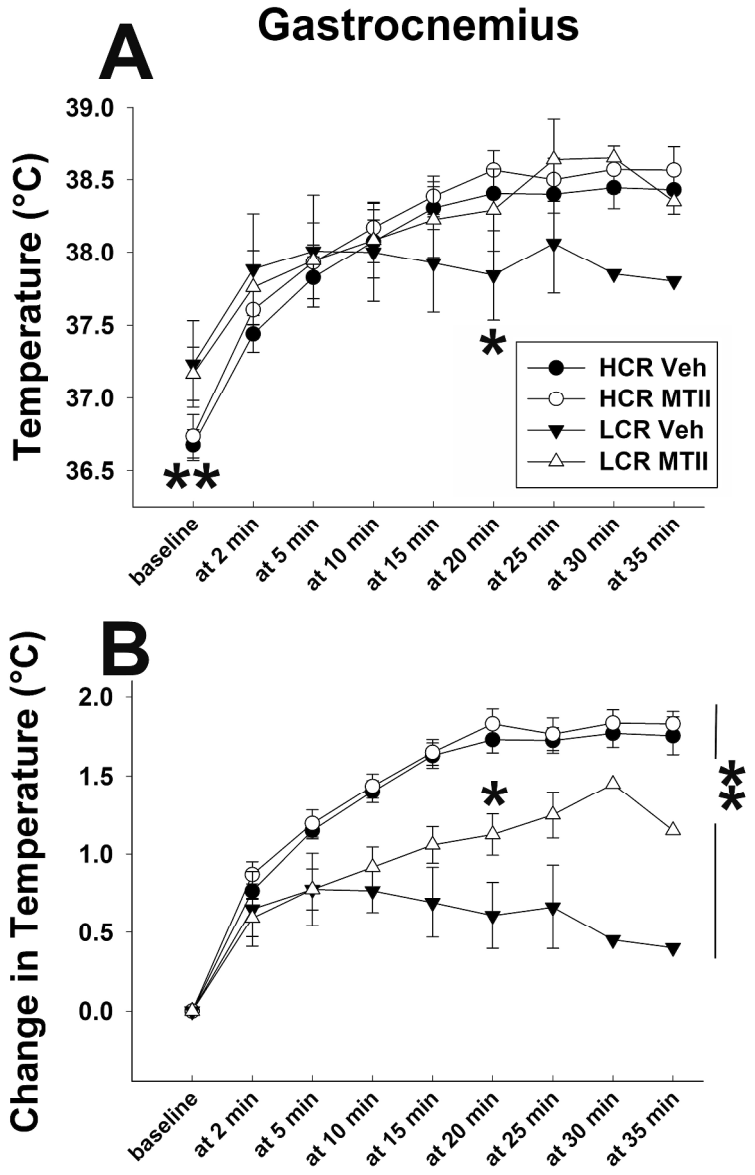

Figure 2: (A) Low and moderate intensity treadmill activity increased skeletal muscle (gastrocnemius) temperature in high-capacity runners (HCR; circles) and low-capacity runners (LCR; triangles) after intra-ventromedial hypothalamic (VMH) microinjections of the mixed melanocortin receptor agonist melanotan II (MTII; open symbols) or vehicle (veh; dark symbols). (B) Walking-induced increase in muscle temperature from baseline were significantly higher in HCR, whereas intra-VMH MTII significantly increased activity-associated muscle heat dissipation in LCR but not HCR. *LCR, MTII treatment significantly different from veh; ** HCR > LCR, main effect (A) and difference at baseline (B); $p<0.05$. (N=10/HCR, 6/LCR)

266x414mm (300 x 300 DPI)

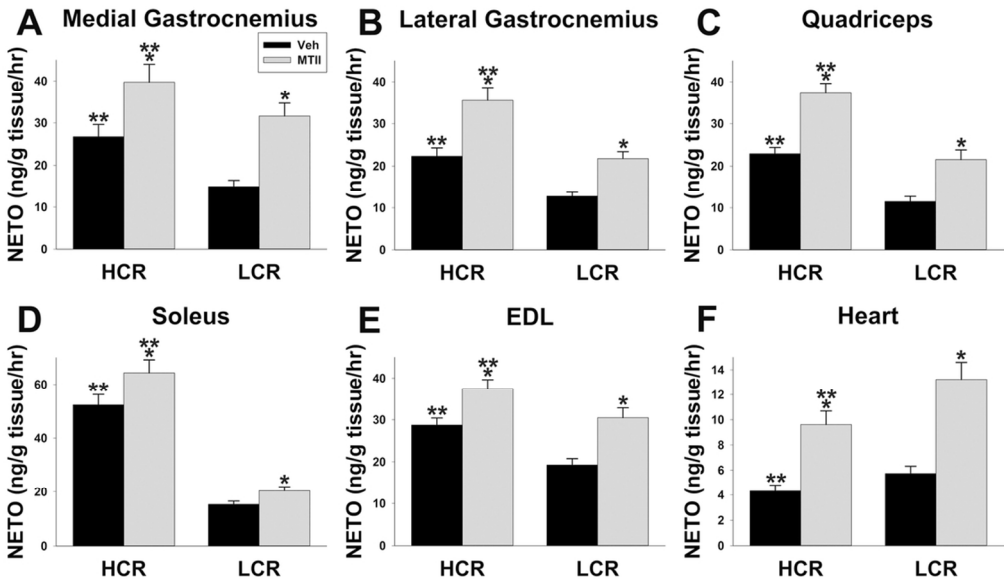

Figure 3: Norepinephrine turnover (NETO) showed differences in sympathetic drive in high- and low-capacity runners (HCR. LCR) after intra-ventromedial hypothalamic (VMH) microinjections of the mixed melanocortin receptor agonist melanotan II (MTII; gray bars) or vehicle (veh; black bars). Intra-VMH MTII significantly increased NETO in skeletal muscle including (A) medial gastrocnemius, (B) lateral gastrocnemius, (C) quadriceps, (D) soleus, and (E) extensor digitorum longus (EDL); HCR showed significantly higher NETO in each of these muscle groups, and also had significantly greater MTII-induced NETO in lateral gastrocnemius, quadriceps, soleus, and EDL. (F) Intra-VMH MTII also increased NETO in heart, but heart NETO was higher in LCR than HCR. *within group, MTII treatment significantly different from veh; **HCR significantly different from LCR within treatment; $p<0.05$. (N=7/HCR, 8/LCR)

100x59mm (300 x 300 DPI)

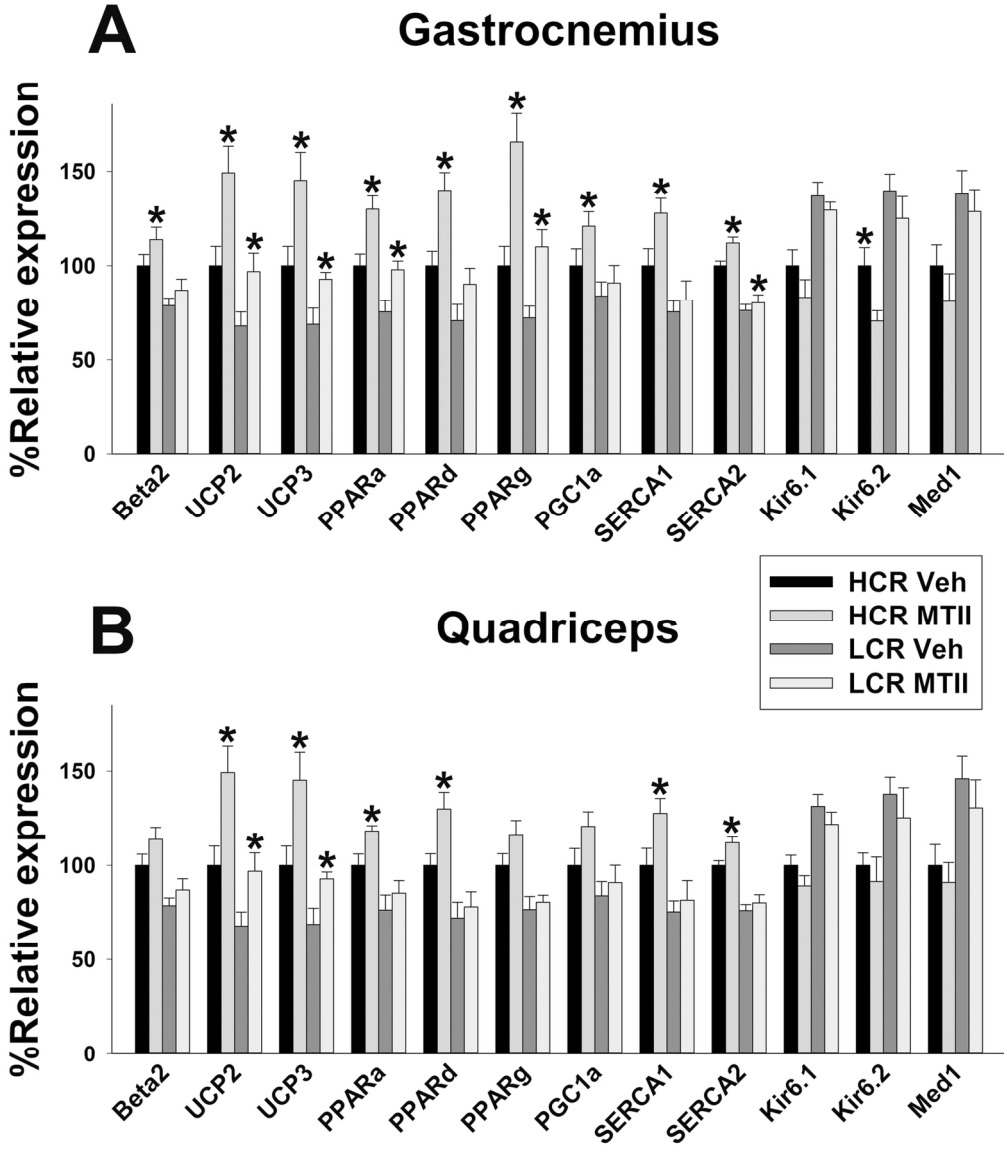

Figure 4: Intra-ventromedial hypothalamic (VMH) microinjections of the melanotan II (MTII) altered mRNA expression of energetic mediators in skeletal muscle (A: medial gastrocnemius; B: quadriceps) in high-and low-capacity runners (HCR, LCR). Beta2: β2 adrenergic receptor; UCP2 and 3: uncoupling protein 2 and 3; PPARa, d, and g: peroxisome proliferator-activated receptor α, δ, and γ; SERCA 1 and 2: sarco/endoplasmic reticulum ATPase 1 and 2; Kir6.1 and 6.1: subunits of the ATP-gated K+ channel, Med1: mediator of RNA polymerase II transcription subunit 1. HCR-MTII ≠ LCR-MTII in all cases. *within group, MTII treatment significantly different from veh; $p<0.05$. (N=8/group)

149x175mm (300 x 300 DPI)

SUPPLEMENTARY MATERIAL

Home-cage gastrocnemius and BAT temperatures after intra-VMH MTII in HCR and LCR.

Hind limb muscle and BAT temperatures were measured at baseline and every 15 min for 240 min after intra-VMH vehicle or MTII microinjection in HCR and LCR. Changes in temperature from individual baseline values were calculated to factor out individual differences in baseline temperature. Intra-VMH MTII induced some change in temperature in BAT in HCR and LCR rats (Figure S1), but was less effective in inducing changes in muscle temperature (Figure S2).

For BAT, there was a small increase in temperature which peaked about one hour after injection. There was a main effect of time but not MTII on BAT temperature, and a significant interaction where the effect of MTII depended on the time after injection. Because of the significant interaction between line and time, HCR and LCR were analyzed separately; in both lines, there was a main effect of MTII and an interaction between MTII and time, where the MTII-induced BAT thermogenesis depended on time since treatment.

There was a significant interaction in change in BAT temperature from baseline where MTII induced a significant deviation from baseline temperature but vehicle microinjection did not. There were also significant main effects of time and MTII, and an interaction between line and time since injection (see Figure S1).

In both the left and right gastrocnemius muscles groups, there was a main effect of time where temperature changed over time. This follows the daily rhythm in baseline muscle temperature we have demonstrated previously (where temperature falls throughout the light phase), which in turn follows the daily rhythm in physical activity levels. There were no main effects of line

(HCR/LCR) or MTII in either the right or left gastrocnemius temperatures. The right gastrocnemius showed a significant interaction where HCR and LCR showed different temperatures depending on the time after injection, but this did not interact with MTII. Similarly, for the mean temperature of both left and right gastrocnemius, there was a main effect of time where mean gastrocnemius temperature changed over time, but no other main effects or interactions.

As shown in Figure S2, when change in gastrocnemius temperature was calculated according to each rat's baseline temperature, there were no significant main effects of line or MTII, but the right gastrocnemius showed a main effect of time where the change in temperature from baseline changed over time (trend in the left gastrocnemius, $p=0.057$). There was a significant MTII-by-time interaction where the right gastrocnemius showed a significant increase in temperature from baseline in the right leg in the latter half of the test, but this did not differ between HCR and LCR. Similarly, for the mean temperature of both left and right gastrocnemius, there was a main effect of time where change in temperature from baseline changed over time, but no other main effects or interactions.

Figure S1.

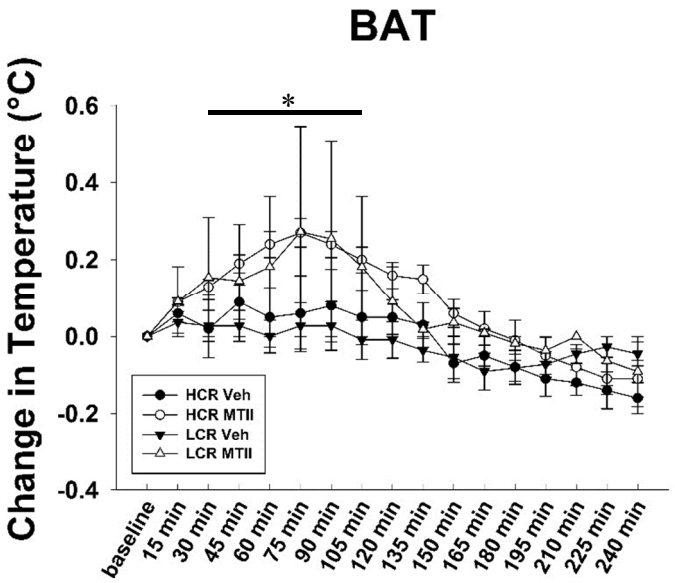

Brown adipose tissue (BAT) change from baseline temperature in high- and low-capacity runners (HCR, LCR) after intra-ventromedial hypothalamic microinjection of vehicle (Veh) or the mixed melanocortin receptor agonist Melanotan II (MTII). Compared to vehicle microinjection, MTII induced a significantly greater increase in temperature above baseline temperature in both HCR (45 min-105 min, and at 150 min after MTII) and LCR (15 min-105 min, and at 165 min after MTII; *$p<0.05$).

Figure S2.

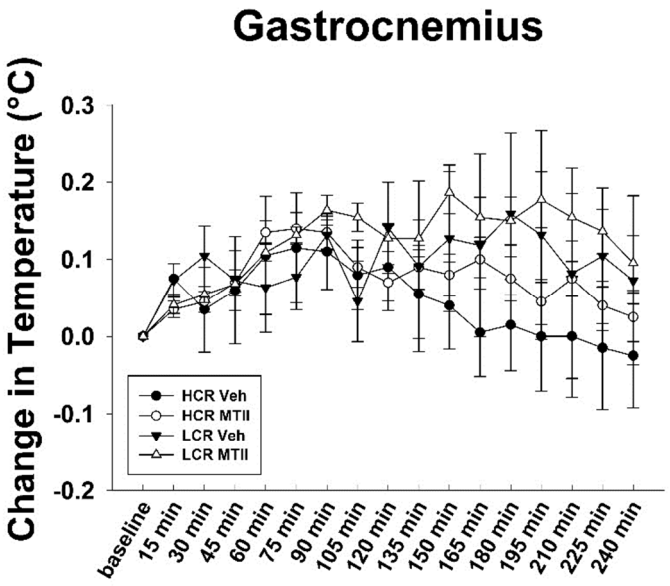

Mean right and left gastrocnemius temperature over 4 hours in the home cage, increase above baseline temperature in high- and low-capacity runners (HCR, LCR) after intra-ventromedial hypothalamic microinjection of vehicle (Veh) or the mixed melanocortin receptor agonist Melanotan II (MTII). The increase in temperature above baseline levels changed over time, but there were not differences between HCR and LCR, and no significant effect of MTII compared to vehicle treatment.

Methods

mRNA and protein expression

Following assay IDs were obtained from IDT technologies for gene expression assays – Gapdh, Rn.PT. 39a.11180736.g; Beta3 adrenergic receptor, Rn.PT.58.35740415; UCP1, Rn.PT.56a.14277400; PPARα, Rn.PT.58.35766078; PPARδ, Rn.PT.58.6572075; PPARγ, Rn.PT.58.6036576; PGC1α, Rn.PT.58.37655048; UCP2, Rn.PT.58.12555837; UCP3, Rn.PT.58.17938212; SERCA1, Rn.PT.58.35312973; SERCA2, Rn.PT.58.8873034; Kir6.1, Rn.PT.58.38199111; Med1, Rn.PT.58.8279221. Probes were diluted as per IDT instructions before proceeding to quantification of gene expression. Data were calculated using ΔCt method and all data are expressed using mean ± SEM relative to HCR vehicle group set at 100%

To evaluate protein expression, primary antibodies against beta 3 adrenergic receptor, UCP1, PPARα, PPARδ, PPARγ, PGC1α, ACC, p-ACC, AMPK, p-AMPK, CD36, FAS, UCP2, beta2 adrenergic receptor, UCP3, SERCA1, SERCA2 (ab101095, ab10983, ab8934, ab23673, ab41928, ab54481, ab45174, ab68191, ab80039, ab133448, ab64014, ab22759, ab67241, ab182136, ab3477, ab2819, ab2861 respectively from Abcam); Kir6.2 and MED1 (sc-11226 and sc-5334 from Santa Cruz), and Kir6.1 (SAB2101220, Sigma-Aldrich) were obtained and incubated with the blot overnight at 4°C and with either anti-rabbit or anti-mouse secondary (ab6721, ab6789 respectively from Abcam) for 1 hr at room temperature. Blots were developed using an Amersham chemiluminescence kit and data expressed as mean ± SEM relative to HCR vehicle group set at 100%.

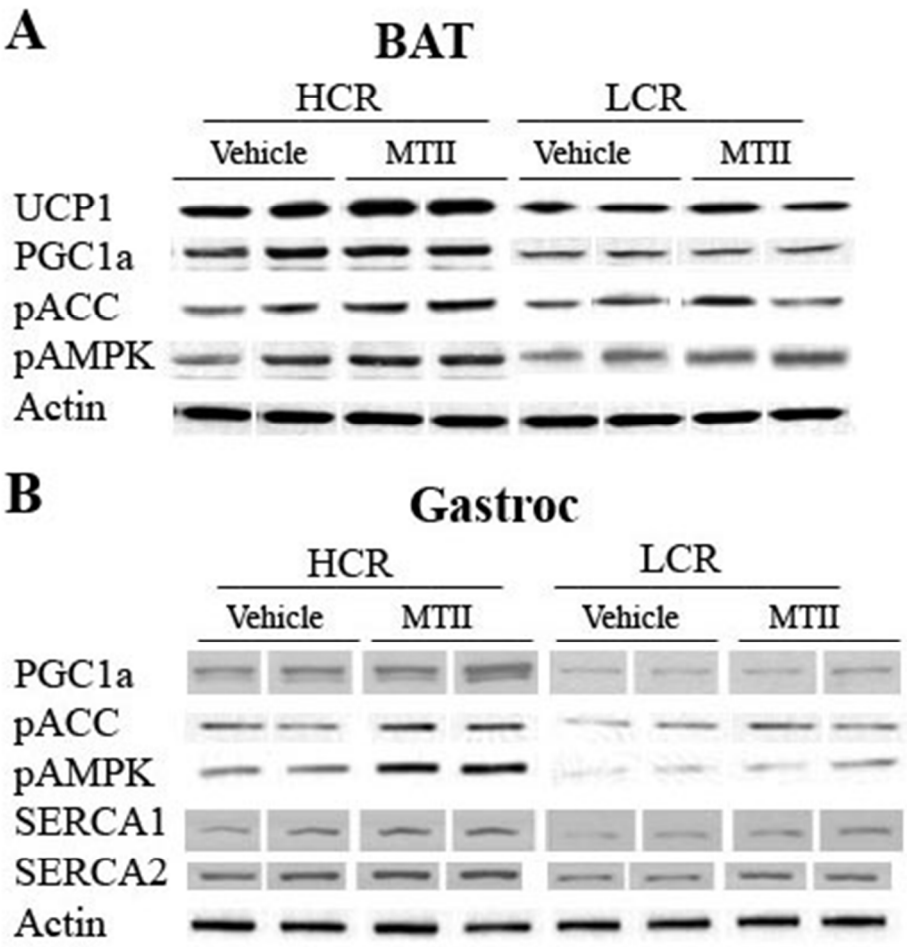

Figure S3. Representative Western blot images of (A) brown adipose tissue (BAT) and (B) gastrocnemius (gastroc) muscle of HCR and LCR treated with either the non-specific melanocortin receptor agonist Melanotan II (MTII) or vehicle (aCSF) in the ventromedial hypothalamus.

Table S1. Body weight and composition in high- and low-capacity runners (HCR, LCR) treated with vehicle (veh) and melanotan II (MTII); Mean±SEM

		HCR			LCR		
Experiment		**vehicle**	**MTII**	percent change	**vehicle**	**MTII**	percent change
Home-cage gastrocnemius & BAT temperature	BW	413.31 ±18.75	410.15 ±18.86	veh>MTII 0.77%	500.11 ±21.15	496.01 ±20.85	veh>MTII 0.83%
4-hr energy expenditure	BW	407.92 ±19.21	410.60 ±18.89		494.13 ±19.79	496.27 ±20.43	
	fat mass	66.99 ±7.49	67.3 ±7.50		106.76 ±11.70	107.5 ±11.49	
	lean mass	252.26 ±10.57	255.44 ±10.70	MTII>veh 1.26%	288.51 ±11.05	286.50 ±11.24	
Treadmill activity thermogenesis	BW	405.63 ±19.28	408.33 ±19.41	MTII>veh 0.67%	487.53 ±26.54	490.19 ±27.92	
	fat mass	68.29 ±7.20	68.76 ±7.22	MTII>veh 0.69%	106.73 ±15.74	107.43 ±16.16	
	lean mass	255.20 ±11.62	256.8 ±11.69	MTII>veh 0.66%	285.3 ±8.62	286.78 ±9.33	
Treadmill activity energy expenditure	BW	401.00 ±18.59	403.64 ±19.52		505.55 ±21.12	500.29 ±20.90	veh>MTII 1.05%
	fat mass	59.48 ±6.84	60.00 ±7.40		114.65 ±13.18	110.27 ±12.48	
	lean mass	251.20 ±10.24	260.61 ±11.51		293.62 ±11.63	283.88 ±10.65	veh>MTII 3.43%

Percent change reported on values that showed significant change between treatments, within line ($p<0.05$). Body weights taken immediately before microinjection; lean and fat mass measured 2 days prior to microinjection. BAT, brown adipose tissue; BW, body weight.

Table S2. Statistical results from analyses examining the effect of intra-ventromedial hypothalamic (VMH) Melanotan II (MTII) and vehicle on gas-exchange variables and physical activity in high- and low-capacity runners (HCR, LCR).

Home-cage energy expenditure			Main effects		Interaction
			MTII/vehicle	HCR/LCR	
	VO_2 (ml/kg/hr)	F	314.85	26.925	20.585
		df	1,19	1,19	1,19
		p	<0.001	<0.001	<0.001
	VCO_2 (ml/kg/hr)	F	244.741	28.812	22.3
		df	1,19	1,19	1,19
		p	<0.001	<0.001	<0.001
	RER	F	43.193	0.031	0.053
		df	1,19	1,19	1,19
		p	<0.001	0.863	0.820
	EE (kcal/hr)	F	323.878	0.668	9.415
		df	1,19	1,19	1,19
		p	<0.001	0.424	0.006
	Horizontal activity counts	F	92.459	9.563	12.292
		df	1,19	1,19	1,19
		p	<0.001	0.006	0.049524
	Ambulatory activity counts	F	63.003	4.263	0.536
		df	1,19	1,19	1,19
		p	<0.001	0.048	0.473
	Vertical activity counts	F	1.145	11.927	0.542
		df	1,19	1,19	1,19
		p	0.707	0.003	0.471
Analysis of covariance					
	EE with body weight as covariate	F	0.224	9.694	15.062
		df	1,17	1,17	1,17
		p	0.642	0.006	0.001
	EE with lean mass as covariate	F	0.657	12.406	8.474
		df	1,17	1,17	1,17
		p	0.429	0.003	0.010
Each covariate was significant, and there were no interactions between treatment (effect of MTII) and covariates					

EE, energy expenditure; RER, respiratory exchange ratio (VCO_2/VO_2).

Table S3. Statistical results from analyses examining the effect of intra-ventromedial hypothalamic (VMH) Melanotan II (MTII) and vehicle on gas-exchange variables in high- and low-capacity runners (HCR, LCR) during treadmill walking activity (walking 7 meters/min for 30 min).

Treadmill energy expenditure			Main effects		Interaction
			MTII/vehicle	**HCR/LCR**	
	VO_2 (ml/kg/hr)	F	27.266	1.604	3.473
		df	1,14	1,14	1,14
		p	<0.001	0.226	0.084
	VCO_2 (ml/kg/hr)	F	0.976	0.081	26.192
		df	1,14	1,14	1,14
		p	0.34	0.781	<0.001
	RER	F	57.619	23.059	5.461
		df	1,14	1,14	1,14
		p	<0.001	<0.001	0.035
	EE (kcal/hr)	F	38.207	7.136	11.114
		df	1,14	1,14	1,14
		p	<0.001	0.018	0.005
Analysis of covariance					
	EE with body weight as covariate	F	0.079	0.198	8.555
		df	1,13	1,13	1,13
		p	0.783	0.664	0.012
	EE with lean mass as covariate	F	0.15	2.342	8.946
		df	1,13	1,13	1,13
		p	0.705	0.15	0.100
Each covariate was significant, and there were no interactions between treatment (effect of MTII) and covariates					

EE, energy expenditure; RER, respiratory exchange ratio (VCO_2/VO_2).

Table S4. Statistical results from analyses examining the effect of intra-ventromedial hypothalamic (VMH) Melanotan II (MTII) and vehicle on gastrocnemius muscle temperature over the course of 4 hrs after treatment in high- and low-capacity runners (HCR, LCR).

Home cage muscle temperature		Main effects			Interactions			
		MTII/vehicle	**Time**	**HCR/LCR**	**Treatment x line**	**Time x line**	**Treatment x time**	**Treatment x time x line**
Right leg temperature	F	0.081	4.330	1.264	0.183	1.682	0.541	0.411
	df	1,19	16,4	1,19	1,19	16,4	16,4	16,4
	p	0.779	<0.001	0.275	0.673	0.049	0.924	0.979
Left leg temperature	F	1.170	1.826	0.693	0.001	1.289	0.924	0.533
	df	1,19	16,4	1,19	1,19	16,4	16,4	16,4
	p	0.393	0.027	0.415	0.975	0.202	0.542	0.929
Average L and R leg temperature	F	0.129	2.622	1.001	0.066	1.610	0.760	0.296
	df	1,19	16,4	1,19	1,19	16,4	16,4	16,4
	p	0.724	0.001	0.330	0.801	0.065	0.730	0.997
Right leg temperature change from baseline	F	2.973	2.939	0.842	0.295	1.354	2.454	0.436
	df	1,19	16,4	1,19	1,19	16,4	16,4	16,4
	p	0.101	<0.001	0.370	0.593	0.164	0.002	0.972
Left leg temperature change from baseline	F	0.091	1.644	1.138	0.338	1.655	0.633	0.359
	df	1,19	16,4	1,19	1,19	16,4	16,4	16,4
	p	0.766	0.057	0.229	0.568	0.055	0.856	0.990
Average R and L leg temperature change from baseline	F	0.550	2.622	1.183	0.003	1.610	0.760	0.296
	df	1,19	16,4	1,19	1,19	16,4	16,4	16,4
	p	0.467	0.001	0.290	0.957	0.065	0.730	0.997
BAT temperature	F	0.260	29.481	0.042	0.372	2.471	5.363	0.503
	df	1,19	16,4	1,19	1,19	16,4	16,4	16,4
	p	0.616	<0.001	0.841	0.549	0.002	p<0.001	0.945
BAT temperature change from baseline	F	8.816	29.481	0.072	0.005	2.471	5.363	0.503
	df	1,19	16,4	1,19	1,19	16,4	16,4	16,4
	p	0.008	<0.001	0.792	0.945	0.002	<0.01	0.945

Table S5. Statistical results from analyses examining the effect of intra-ventromedial hypothalamic (VMH) Melanotan II (MTII) and vehicle on gastrocnemius muscle temperature during treadmill walking in high- and low-capacity runners (HCR, LCR).

Treadmill-activity muscle temperature		Main effects			Interactions			
		MTII/vehicle	**Time**	**HCR/LCR**	**Treatment x line**	**Time x line**	**Treatment x time**	**Treatment x time x line**
Right leg temperature	F	1.470	127.156	0.016	0.007	20.176	3.773	3.524
	df	1,14	5,10	1,14	1,14	5,10	5,10	5,10
	p	0.245	<0.001	0.900	0.933	<0.001	0.004	0.007
Left leg temperature	F	0.224	199.702	0.091	0.001	19.409	3.161	2.534
	df	1,14	5,10	1,14	1,14	5,10	5,10	5,10
	p	0.643	<0.001	0.767	0.971	<0.001	0.120	0.036
Average L and R leg temperature	F	0.860	190.009	0.006	0.005	24.529	4.772	4.219
	df	1,14	5,10	1,14	1,14	5,10	5,10	5,10
	p	0.370	<0.001	0.937	0.947	<0.001	0.001	0.002
Right leg temperature change from baseline	F	0.878	127.165	16.039	0.878	20.176	3.773	3.524
	df	1,14	5,10	1,14	1,14	5,10	5,10	5,10
	p	0.365	<0.001	0.001	0.365	<0.001	0.004	0.007
Left leg temperature change from baseline	F	2.754	199.702	17.345	0.172	19.409	3.161	2.534
	df	1,14	5,10	1,14	1,14	5,10	5,10	5,10
	p	0.119	<0.001	0.001	0.685	<0.001	0.120	0.036
Average R and L leg temperature change from baseline	F	2.577	199.009	18.920	0.706	24.529	4.772	4.219
	df	1,14	5,10	1,14	1,14	5,10	5,10	5,10
	p	0.131	<0.001	0.001	0.415	<0.001	0.001	0.002
BAT temperature (before and after activity)	F	1.170	11.051	1.061	1.453	10.000	2.133	0.050
	df	1,14	1,14	1,14	1,14	1,14	1,14	1,14
	p	0.231	<0.001	0.320	0.248	0.007	0.166	0.825
BAT temperature change from baseline	F	2.133	N/A	10.000	0.050	N/A	N/A	N/A
	df	1,14		1,14	1,14			
	p	0.166		0.007	0.825			

Analysis included temperatures though 20 min of treadmill walking to encompass data for all rats, before any rats became noncompliant with treadmill-waling protocol. BAT temperatures were measured once before and once after treadmill walking (significant decrease over time, larger decrease in HCR).

Norepinephrine turnover (NETO)		Main effects		Interaction
		MTII/vehicle	HCR/LCR	
BAT	F	572.245	52.627	127.835
	df	1,13	1,13	1,13
	p	<0.001	<0.001	<0.001
MWAT	F	115.306	21.661	27.274
	df	1,13	1,13	1,13
	p	<0.001	<0.001	<0.001
RWAT	F	160.033	1.961	1.116
	df	1,13	1,13	1,13
	p	<0.001	0.183	0.309
EWAT	F	309.205	11.503	11.883
	df	1,13	1,13	1,13
	p	<0.001	0.004	0.004
GWAT	F	314.589	13.91	202.977
	df	1,13	1,13	1,13
	p	<0.001	0.002	<0.001
IWAT	F	258.613	8.474	65.392
	df	1,13	1,13	1,13
	p	<0.001	0.012	<0.001
Liver	F	107.912	7.332	19.324
	df	1,13	1,13	1,13
	p	<0.001	0.018	0.001
Heart	F	166.185	3.935	4.952
	df	1,13	1,13	1,13
	p	<0.001	0.069	0.044
Soleus	F	276.059	70.096	46.498
	df	1,13	1,13	1,13
	p	<0.001	<0.001	<0.001
EDL	F	392.559	9.193	6.119
	df	1,13	1,13	1,13
	p	<0.001	0.009	0.027
Quadriceps	F	298.337	36.944	9.053
	df	1,13	1,13	1,13
	p	<0.001	<0.001	0.009
Lateral gastrocnemius	F	290.798	17.969	10.142
	df	1,13	1,13	1,13
	p	<0.001	0.001	0.007
Medial gastrocnemius	F	193.457	5.539	2.903
	df	1,13	1,13	1,13
	p	<0.001	0.034	0.110

Table S6. Statistical results from analyses examining the effect of intra-ventromedial hypothalamic (VMH) Melanotan II (MTII) and vehicle on norepinephrine turnover (NETO) in high- and low-capacity runners (HCR, LCR.

BAT, brown adipose tissue; MWAT, mesenteric white adipose tissue; RWAT, retroperitoneal white adipose tissue; EWAT, epididymal white adipose tissue; GWAT, gluteal white adipose tissue; IWAT, inguinal white adipose tissue; EDL, extensor digitorum longus.

Table S7. Statistical results from analyses examining the effect of intra-ventromedial hypothalamic (VMH) Melanotan II (MTII) and vehicle on brown adipose tissue (BAT) mRNA expression using qPCR in high- and low-capacity runners (HCR, LCR).

Brown adipose tissue (BAT)		Main effects		Interaction	t-test for MTII≠vehicle	
		MTII/vehicle	HCR/LCR		HCR	LCR
β3-AR	F	0.376	3.527	0.272		
	df	1,28	1,28	1,28		
	p	0.544	0.071	0.606	0.480	0.102
UCP1	F	19.477	60.218	1.437		
	df	1,28	1,28	1,28		
	p	<0.001	<0.001	0.241	0.001	0.020
PPARα	F	19.502	37.072	1.892		
	df	1,28	1,28	1,28		
	p	<0.001	<0.001	0.18	0.002	0.008
PPARδ	F	31.913	37.072	0.112		
	df	1,28	1,28	1,28		
	p	<0.001	<0.001	0.74	0.000	0.024
PPARγ	F	23.261	46.191	1.736		
	df	1,28	1,28	1,28		
	p	<0.001	<0.001	0.198	0.000	0.033
PGC1α	F	21.241	37.49	2.907		
	df	1,28	1,28	1,28		
	p	<0.001	<0.001	0.099	0.001	0.007

β3-AR, Beta-3 adrenergic receptor; UCP1, uncoupling protein 1; PPAR, peroxisome proliferator activated receptor; PGC1α, PPARγ coactivator-1α.

Table S8. Statistical results from analyses examining the effect of intra-ventromedial hypothalamic (VMH) Melanotan II (MTII) and vehicle on white adipose tissue (WAT) mRNA expression using qPCR in high- and low-capacity runners (HCR, LCR).

White adipose tissue (WAT)		Main effects		Interaction	t-test for MTII≠vehicle	
		MTII/vehicle	HCR/LCR		HCR	LCR
β3-AR	F	4.877	22.009	0.375		
	df	1,28	1,28	1,28		
	p	0.36	<0.001	0.545	0.050	0.101
UCP2	F	2.184	37.707	0.168		
	df	1,28	1,28	1,28		
	p	0.151	<0.001	0.685	0.129	0.194
PPARα	F	22.384	37.856	0.536		
	df	1,28	1,28	1,28		
	p	<0.001	<0.001	0.47	0.002	0.003
PPARδ	F	31.913	37.072	0.112		
	df	1,28	1,28	1,28		
	p	<0.001	<0.001	0.74	0.001	0.000
PPARγ	F	14.813	31.963	1.163		
	df	1,28	1,28	1,28		
	p	0.001	<0.001	0.29	0.005	0.012
PGC1α	F	2.235	31.472	0.473		
	df	1,28	1,28	1,28		
	p	0.146	<0.001	0.497	0.066	0.295

β3-AR, Beta-3 adrenergic receptor; UCP2, uncoupling protein 2; PPAR, peroxisome proliferator activated receptor; PGC1α, PPARγ coactivator-1α.

Table S9. Statistical results from analyses examining the effect of intra-ventromedial hypothalamic (VMH) Melanotan II (MTII) and vehicle on liver mRNA expression using qPCR in high- and low-capacity runners (HCR, LCR).

Liver		Main effects		Interaction	t-test for MTII≠vehicle	
		MTII/vehicle	HCR/LCR		HCR	LCR
β2-AR	F	8.913	13.8	0.056		
	df	1,28	1,28	1,28		
	p	0.006	0.001	0.814	0.042	0.016
UCP2	F	14.544	20.254	1.239		
	df	1,28	1,28	1,28		
	p	0.001	<0.001	0.275	0.002	0.033
PPARα	F	31.701	18.427	1.608		
	df	1,28	1,28	1,28		
	p	<0.001	<0.001	0.215	0.001	0.000
PPARδ	F	74.835	48.171	6.878		
	df	1,28	1,28	1,28		
	p	<0.001	<0.001	0.014	0.000	0.000
PPARγ	F	31.376	15.815	1.938		
	df	1,28	1,28	1,28		
	p	<0.001	<0.001	0.175	0.001	0.001
PGC1α	F	52.246	28.808	1.814		
	df	1,28	1,28	1,28		
	p	<0.001	<0.001	0.189	0.000	0.000

B2-AR, Beta-2 adrenergic receptor; UCP2, uncoupling protein 2; PPAR, peroxisome proliferator activated receptor; PGC1α, PPARγ coactivator-1α.

Table S10. Statistical results from analyses examining the effect of intra-ventromedial hypothalamic (VMH) Melanotan II (MTII) and vehicle on gastrocnemius mRNA expression using qPCR in high- and low-capacity runners (HCR, LCR).

Gastrocnemius		Main effects		Interaction	t-test for MTII≠vehicle	
		MTII/vehicle	HCR/LCR		HCR	LCR
β2-AR	F	9.498	22.179	2.201		
	df	1,28	1,28	1,28		
	p	0.005	<0.001	0.149	0.009	0.069
UCP2	F	13.382	19.927	0.388		
	df	1,28	1,28	1,28		
	p	0.001	<0.001	0.536	0.014	0.003
UCP3	F	23.574	15.735	0.293		
	df	1,28	1,28	1,28		
	p	<0.001	<0.001	0.592	0.002	0.002
PPARα	F	14.728	17.598	0.31		
	df	1,28	1,28	1,28		
	p	0.001	<0.001	0.582	0.003	0.020
PPARδ	F	13.702	23.685	1.572		
	df	1,28	1,28	1,28		
	p	0.001	<0.001	0.22	0.004	0.030
PPARγ	F	22.747	15.151	1.714		
	df	1,28	1,28	1,28		
	p	<0.001	0.001	0.201	0.001	0.003
PGC1α	F	9.778	13.544	0.474		
	df	1,28	1,28	1,28		
	p	0.004	0.001	0.497	0.016	0.030
SERCA1	F	11.077	25.884	2.067		
	df	1,28	1,28	1,28		
	p	<0.001	<0.001	0.162	0.003	0.095
SERCA2	F	19.816	15.613	1.93		
	df	1,28	1,28	1,28		
	p	<0.001	<0.001	0.176	0.003	0.001
Kir6.1	F	3.269	38.247	0.484		
	df	1,28	1,28	1,28		
	p	0.081	<0.001	0.492	0.059	0.206
Kir6.2	F	9.39	42.931	1.001		
	df	1,28	1,28	1,28		
	p	0.005	<0.001	0.326	0.003	0.102
MED1	F	2.071	18.853	0.268		
	df	1,28	1,28	1,28		
	p	0.161	<0.001	0.609	0.118	0.233

Muscle abbreviations (Tables S10-S11):

B2-AR, Beta-2 adrenergic receptor; UCP2 and 3, uncoupling protein 2 and 3; PPAR, peroxisome proliferator activated receptor; PGC1α, PPARγ coactivator-1α; SERCA, sarco/endoplasmic reticulum Ca^{2+}-ATPase; Kir6.1 and 6.2, components of ATP-gated K^{+}-channel; MED1, Mediator of RNA polymerase II transcription subunit 1.

Table S11. Statistical results from analyses examining the effect of intra-ventromedial hypothalamic (VMH) Melanotan II (MTII) and vehicle on quadriceps mRNA expression using qPCR in high- and low-capacity runners (HCR, LCR).

Quadriceps		Main effects		Interaction	t-test for MTII≠vehicle	
		MTII/vehicle	HCR/LCR		HCR	LCR
β2-AR	F	4.352	20.736	0.269		
	df	1,28	1,28	1,28		
	p	0.046	<0.001	0.608	0.056	0.121
UCP2	F	15.45	18.064	1.042		
	df	1,28	1,28	1,28		
	p	0.001	<0.001	0.316	0.007	0.004
UCP3	F	18.581	27.072	1.723		
	df	1,28	1,28	1,28		
	p	<0.001	<0.001	0.2	0.004	0.002
PPARα	F	7.746	32.282	0.855		
	df	1,28	1,28	1,28		
	p	0.01	<0.001	0.363	0.006	0.121
PPARδ	F	7.163	35.755	3.233		
	df	1,28	1,28	1,28		
	p	0.012	<0.001	0.083	0.006	0.253
PPARγ	F	3.829	31.905	1.311		
	df	1,28	1,28	1,28		
	p	0.06	<0.001	0.262	0.034	0.261
PGC1α	F	3.86	10.493	0.926		
	df	1,28	1,28	1,28		
	p	0.059	0.003	0.344	0.033	0.237
SERCA1	F	5.653	24.607	2.303		
	df	1,28	1,28	1,28		
	p	0.024	<0.001	0.14	0.010	0.266
SERCA2	F	4.886	57.654	1.1		
	df	1,28	1,28	1,28		
	p	0.035	<0.001	0.303	0.005	0.250
Kir6.1	F	3.206	31.955	0.017		
	df	1,28	1,28	1,28		
	p	0.084	<0.001	0.897	0.069	0.156
Kir6.2	F	1.401	16.331	0.046		
	df	1,28	1,28	1,28		
	p	0.246	<0.001	0.832	0.273	0.139
MED1	F	1.304	16.024	0.084		
	df	1,28	1,28	1,28		
	p	0.263	<0.001	0.774	0.261	0.182

Table S12. Statistical results from analyses examining the effect of intra-ventromedial hypothalamic (VMH) Melanotan II (MTII) and vehicle on brown adipose tissue (BAT) protein expression using Western blot in high- and low-capacity runners (HCR, LCR).

Brown adipose tissue (BAT)		Main effects		Interaction	t-test for MTII≠vehicle	
		MTII/vehicle	HCR/LCR		HCR	LCR
β3-AR	F	2.644	11.725	0.192		
	df	1,10	1,10	1,10		
	p	0.135	0.007	0.671	0.258	0.054
UCP1	F	9.374	62.4	0.914		
	df	1,10	1,10	1,10		
	p	0.012	<0.001	0.362	0.009	0.125
PPARα	F	2.02	3.82	0.202		
	df	1,10	1,10	1,10		
	p	0.186	0.079	0.663	0.140	0.240
PPARδ	F	1.029	1.575	0.05		
	df	1,10	1,10	1,10		
	p	0.334	0.238	0.827	0.203	0.306
PPARγ	F	1.405	9.053	0.037		
	df	1,10	1,10	1,10		
	p	0.263	0.013	0.851	0.244	0.200
PGC1α	F	5.018	18.86	1.036		
	df	1,10	1,10	1,10		
	p	0.049	0.001	0.333	0.023	0.236
ACC	F	0.000	0.416	0.005		
	df	1,10	1,10	1,10		
	p	0.983	0.533	0.945	0.485	0.477
pACC	F	10.578	10.765	2.114		
	df	1,10	1,10	1,10		
	p	0.009	0.008	0.176	0.013	0.115
AMPK	F	0.039	0.053	0.000		
	df	1,10	1,10	1,10		
	p	0.847	0.822	0.996	0.438	0.453
pAMPK	F	14.061	16.655	1.558		
	df	1,10	1,10	1,10		
	p	0.004	0.002	0.24	0.008	0.069
CD36 (FAT)	F	0.24	1.324	0.016		
	df	1,10	1,10	1,10		
	p	0.635	0.277	0.903	0.412	0.323
FAS	F	0.037	0.02	0.000		
	df	1,10	1,10	1,10		
	p	0.852	0.89	0.992	0.447	0.450

Table S12 abbreviations:

B3-AR, Beta-3 adrenergic receptor; UCP1, uncoupling protein 1; PPAR, peroxisome proliferator activated receptor; PGC1α, PPARγ coactivator-1α; (p)ACC, (phosphor-)acetyl-CoA carboxylase; (p)AMPK, (phospho-)AMP-activated protein kinase; CD36, fatty acid translocase; FAS, fatty acid synthase.

Table S13. Statistical results from analyses examining the effect of intra-ventromedial hypothalamic (VMH) Melanotan II (MTII) and vehicle on white adipose tissue (WAT) protein expression using Western blot in high- and low-capacity runners (HCR, LCR).

White adipose tissue (WAT)		Main effects		Interaction	t-test for MTII≠vehicle	
		MTII/vehicle	HCR/LCR		HCR	LCR
β3-AR	F	1.87	15.865	0.089		
	df	1,10	1,10	1,10		
	p	0.201	0.003	0.772	0.135	0.251
UCP2	F	0.852	5.761	0.052		
	df	1,10	1,10	1,10		
	p	0.378	0.037	0.824	0.239	0.311
PPARα	F	1.446	1.677	0.000		
	df	1,10	1,10	1,10		
	p	0.257	0.224	0.996	0.151	0.256
PPARδ	F	0.127	0.056	0.001		
	df	1,10	1,10	1,10		
	p	0.729	0.817	0.971	0.408	0.400
PPARγ	F	2.453	2.831	0.11		
	df	1,10	1,10	1,10		
	p	0.148	0.123	0.747	0.098	0.230
PGC1α	F	2.448	6.458	0.108		
	df	1,10	1,10	1,10		
	p	0.149	0.029	0.749	0.105	0.225
ACC	F	0.003	0.479	0.000		
	df	1,10	1,10	1,10		
	p	0.959	0.505	1.000	0.486	0.486
pACC	F	4.04	1.222	0.000		
	df	1,10	1,10	1,10		
	p	0.072	0.297	0.988	0.110	0.105
AMPK	F	0.012	0.007	0.003		
	df	1,10	1,10	1,10		
	p	0.916	0.936	0.956	0.487	0.454
pAMPK	F	7.565	1.962	1.301		
	df	1,10	1,10	1,10		
	p	0.02	0.192	0.281	0.023	0.144
CD36 (FAT)	F	0.003	0.543	0.000		
	df	1,10	1,10	1,10		
	p	0.954	0.478	0.997	0.484	0.484
FAS	F	0.19	0.168	0.013		
	df	1,10	1,10	1,10		
	p	0.672	0.69	0.912	0.352	0.417

Table S13 abbreviations:

B3-AR, Beta-3 adrenergic receptor; UCP2, uncoupling protein 2; PPAR, peroxisome proliferator activated receptor; PGC1α, PPARγ coactivator-1α; (p)ACC, (phosphor-)acetyl-CoA carboxylase; (p)AMPK, (phospho-)AMP-activated protein kinase; CD36, fatty acid translocase; FAS, fatty acid synthase.

Table S14. Statistical results from analyses examining the effect of intra-ventromedial hypothalamic (VMH) Melanotan II (MTII) and vehicle on liver protein expression using Western blot in high- and low-capacity runners (HCR, LCR).

Liver		Main effects		Interaction	t-test for MTII≠vehicle	
		MTII/vehicle	HCR/LCR		HCR	LCR
β2-AR	F	1.715	9.737	0.131		
	df	1,10	1,10	1,10		
	p	0.22	0.011	0.725	0.283	0.123
UCP2	F	2.294	16.113	0.067		
	df	1,10	1,10	1,10		
	p	0.161	0.002	0.802	0.152	0.183
PPARα	F	3.693	4.178	0.096		
	df	1,10	1,10	1,10		
	p	0.084	0.068	0.763	0.110	0.121
PPARδ	F	4.3	11.853	0.629		
	df	1,10	1,10	1,10		
	p	0.065	0.006	0.446	0.054	0.194
PPARγ	F	3.628	17.526	0.265		
	df	1,10	1,10	1,10		
	p	0.086	0.002	0.618	0.054	0.209
PGC1α	F	0.693	10.01	0.521		
	df	1,10	1,10	1,10		
	p	0.425	0.01	0.487	0.181	0.467
AMPK	F	0.000	0.013	0.001		
	df	1,10	1,10	1,10		
	p	0.986	0.912	0.978	0.487	0.497
pAMPK	F	6.219	10.559	2.052		
	df	1,10	1,10	1,10		
	p	0.032	0.009	0.182	0.019	0.246
CD36 (FAT)	F	0.427	7.195	0.085		
	df	1,10	1,10	1,10		
	p	0.528	0.023	0.776	0.275	0.400
FAS	F	0.003	0.085	0.031		
	df	1,10	1,10	1,10		
	p	0.955	0.776	0.865	0.438	0.469

Table S14 abbreviations:

B3-AR, Beta-3 adrenergic receptor; UCP1, uncoupling protein 1; PPAR, peroxisome proliferator activated receptor; PGC1α, PPARγ coactivator-1α; (p)AMPK, (phospho-)AMP-activated protein kinase; CD36, fatty acid translocase; FAS, fatty acid synthase.

Table S15. Statistical results from analyses examining the effect of intra-ventromedial hypothalamic (VMH) Melanotan II (MTII) and vehicle on gastrocnemius protein expression using Western blot in high- and low-capacity runners (HCR, LCR).

Gastrocnemius		Main effects		Interaction	t-test for MTII≠vehicle	
		MTII/vehicle	HCR/LCR		HCR	LCR
β2-AR	F	3.07	21.328	0.347		
	df	1,10	1,10	1,10		
	p	0.11	0.001	0.569	0.073	0.232
UCP2	F	1.019	23.156	0.131		
	df	1,10	1,10	1,10		
	p	0.337	0.001	0.725	0.183	0.337
UCP3	F	1.5585	27.783	0.572		
	df	1,10	1,10	1,10		
	p	0.237	<0.001	0.467	0.112	0.365
PPARα	F	2.658	18.262	0.006		
	df	1,10	1,10	1,10		
	p	0.134	0.002	0.941	0.157	0.142
PPARδ	F	3.653	18.654	0.089		
	df	1,10	1,10	1,10		
	p	0.085	0.002	0.771	0.106	0.130
PPARγ	F	4.359	20.371	0.517		
	df	1,10	1,10	1,10		
	p	0.063	0.001	0.489	0.059	0.177
PGC1α	F	5.534	31.995	1.272		
	df	1,10	1,10	1,10		
	p	0.04	<0.001	0.286	0.023	0.226
SERCA1	F	5.843	31.356	0.581		
	df	1,10	1,10	1,10		
	p	0.036	<0.001	0.463	0.026	0.169
SERCA2	F	3.609	42.549	0.991		
	df	1,10	1,10	1,10		
	p	0.087	<0.001	0.343	0.051	0.271
Kir6.1	F	0.161	12.388	0.000		
	df	1,10	1,10	1,10		
	p	0.697	0.006	0.998	0.384	0.402
Kir6.2	F	0.057	27.232	0.037		
	df	1,10	1,10	1,10		
	p	0.817	<0.001	0.851	0.377	0.489
MED1	F	0.085	33	0.057		
	df	1,10	1,10	1,10		
	p	0.777	<0.001	0.816	0.487	0.357

Table S15-S16 abbreviations:

B2-AR, Beta-2 adrenergic receptor; UCP2 and 3, uncoupling protein 2 and 3; PPAR, peroxisome proliferator activated receptor; PGC1α, PPARγ coactivator-1α; SERCA, sarco/endoplasmic reticulum Ca^{2+}-ATPase; Kir6.1 and 6.2, components of ATP-gated K^{+}-channel; MED1, Mediator of RNA polymerase II transcription subunit 1; (p)AMPK, (phospho-)AMP-activated protein kinase; CD36, fatty acid translocase; FAS, fatty acid synthase.

ACC	F	0.118	1.134	0.102		
	df	1,10	1,10	1,10		
	p	0.738	0.312	0.756	0.494	0.321
pACC	F	10.516	28.566	0.986		
	df	1,10	1,10	1,10		
	p	0.009	<0.001	0.344	0.015	0.086
AMPK	F	0.002	0.012	0.001		
	df	1,10	1,10	1,10		
	p	0.965	0.917	0.973	0.479	0.497
pAMPK	F	11.619	25.222	0.757		
	df	1,10	1,10	1,10		
	p	0.007	0.001	0.405	0.012	0.074
CD36 (FAT)	F	2.41	14.068	0.156		
	df	1,10	1,10	1,10		
	p	0.152	0.004	0.701	0.114	0.224
FAS	F	0.04	1.211	0.024		
	df	1,10	1,10	1,10		
	p	0.845	0.297	0.879	0.408	0.488

Table S16. Statistical results from analyses examining the effect of intra-ventromedial hypothalamic (VMH) Melanotan II (MTII) and vehicle on quadriceps protein expression using Western blot in high- and low-capacity runners (HCR, LCR).

Quadriceps		Main effects		Interaction	t-test for MTII≠vehicle	
		MTII/vehicle	HCR/LCR		HCR	LCR
β2-AR	F	0.633	7.983	0.027		
	df	1,10	1,10	1,10		
	p	0.445	0.018	0.872	0.275	0.327
UCP2	F	0.494	23.761	0.118		
	df	1,10	1,10	1,10		
	p	0.498	0.001	0.739	0.251	0.402
UCP3	F	0.766	24.987	0.263		
	df	1,10	1,10	1,10		
	p	0.402	0.001	0.619	0.198	0.398
PPARα	F	0.731	6.775	0.078		
	df	1,10	1,10	1,10		
	p	0.413	0.026	0.785	0.245	0.338
PPARδ	F	0.02	6.22	0.066		
	df	1,10	1,10	1,10		
	p	0.89	0.032	0.802	0.401	0.467
PPARγ	F	1.151	10.182	0.303		
	df	1,10	1,10	1,10		
	p	0.173	0.01	0.594	0.126	0.249

PGC1α	F	2.279	30.836	0.196		
	df	1,10	1,10	1,10		
	p	0.162	<0.001	0.667	0.109	0.246
SERCA1	F	3.919	19.141	0.397		
	df	1,10	1,10	1,10		
	p	0.076	0.001	0.543	0.047	0.212
SERCA2	F	2.538	20.539	0.13		
	df	1,10	1,10	1,10		
	p	0.142	0.001	0.726	0.116	0.208
Kir6.1	F	0.118	3.612	0.01		
	df	1,10	1,10	1,10		
	p	0.739	0.087	0.923	0.418	0.400
Kir6.2	F	0.405	24.289	0.000		
	df	1,10	1,10	1,10		
	p	0.539	0.001	0.985	0.336	0.335
MED1	F	0.216	32.532	0.024		
	df	1,10	1,10	1,10		
	p	0.652	<0.001	0.881	0.415	0.344
ACC	F	0.162	0.877	0.020		
	df	1,10	1,10	1,10		
	p	0.695	0.731	0.890	0.435	0.346
pACC	F	3.077	5.656	0.330		
	df	1,10	1,10	1,10		
	p	0.110	0.039	0.578	0.081	0.220
AMPK	F	0.010	0.000	0.000		
	df	1,10	1,10	1,10		
	p	0.923	0.991	0.995	0.472	0.474
pAMPK	F	6.679	20.554	0.300		
	df	1,10	1,10	1,10		
	p	0.027	0.001	0.596	0.041	0.101
CD36 (FAT)	F	0.081	6.323	0.039		
	df	1,10	1,10	1,10		
	p	0.782	0.031	0.847	0.369	0.477
FAS	F	0.002	0.002	0.024		
	df	1,10	1,10	1,10		
	p	0.966	0.964	0.880	0.452	0.466